Received: 23 June 2020 | Accepted: 9 September 2020

DOI: 10.1111/jfb.14538

REGULAR PAPER

JOURNAL OF FISH BIOLOGY fsbi

# Species delimitation in a range-restricted group of cascudinhos (Loricariidae: *Epactionotus*) supports morphological and genetic differentiation across coastal rivers of southern Brazil

Maria Laura S. Delapieve[1] | Tiago P. Carvalho[2] | Roberto E. Reis[1]

[1]Laboratory of Vertebrate Systematics, Pontifícia Universidade Católica do Rio Grande do Sul, PUCRS, Porto Alegre, Brazil

[2]Laboratorio de Ictiología, Unidad de Ecología y Sistemática (UNESIS), Departamento de Biología, Facultad de Ciencias, Pontificia Universidad Javeriana, Bogotá, Colombia

**Correspondence**
Maria Laura S. Delapieve, Laboratory of Vertebrate Systematics, Pontifícia Universidade Católica do Rio Grande do Sul, PUCRS, Av. Ipiranga 6681, 90619-900 Porto Alegre, RS, Brazil.
Email: laura.delapieve@gmail.com

**Funding information**
Conselho Nacional de Desenvolvimento Científico e Tecnológico; Coordenação de Aperfeiçoamento de Pessoal de Nível Superior

## Abstract

*Epactionotus* species are known for inhabiting the rocky-bottom stretches of fast-flowing rivers in a limited geographic area along the Atlantic coast of southern Brazil. These species are endemic to single coastal river drainages (two neighbouring drainages for *Epactionotus bilineatus*) isolated from each other by the coastal lacustrine environments or the Atlantic Ocean. *E. bilineatus* is from the Maquiné and Três Forquilhas River basins, both tributaries of the Tramandaí River system, whereas *E. itaimbezinho* is endemic to the Mampituba River drainage and *Epactionotus gracilis* to the Araranguá River drainage. Recent fieldwork in the Atlantic coastal drainages of southern Brazil revealed new populations in the Urussanga, Tubarão, d'Una and Biguaçu River drainages. Iterative species delimitation using molecular data (cytochrome c oxidase subunit I) and morphology (morphometrics and meristics) was applied to evaluate species recognition of isolated populations. With regard to new data, the genus was re-diagnosed, the status of *Epactionotus* species/populations was re-evaluated, formerly described species were supported and population structure was recognized. As for the newly discovered populations, both morphological and molecular data strongly support the population from the Biguaçu River drainage, in Santa Catarina State, as a new species. Molecular data revealed strong per-basin population structure, which may be related to species habitat specificity and low or no dispersal among drainages.

KEYWORDS

coastal Brazilian drainages, *col* gene, genetic distance, Hypoptopomatinae, iterative taxonomy, Neotropical fish

## 1 | INTRODUCTION

Species of the cascudinho genus *Epactionotus* Reis & Schaefer, 1998, were originally described from a limited geographic area along the Atlantic coast of southern Brazil. River drainages included in this region are part of the Tramandaí–Mampituba freshwater ecoregion (Abell *et al*., 2008 – FEOW 335), and records of this genus were, until recently, exclusive to this freshwater ecoregion. This ecoregion contains many endemic species (Albert *et al*., 2011; Ferrer *et al*., 2015; Malabarba & Isaia, 1992; Reis & Schaefer, 1998) and has a relatively well-known species diversity (Bertaco *et al*., 2016). The area has been a stage for recent studies testing phylogeographic questions associated with Pleistocene sea-level changes and ecologically mediated dispersal, as well as species delimitation based on both morphological and molecular data (Angrizani & Malabarba, 2018; Hirschmann *et al*., 2015, 2017; Thomaz *et al*., 2015, 2017).

*Epactionotus* species are usually found in rocky-bottom stretches of rivers, inhabiting fast-flowing waters, and each of its three species

  

is endemic to a single river drainage (except for *Epactionotus bilineatus*), which are isolated from each other by the Atlantic Ocean or coastal lacustrine systems (Figure 1; Supporting Information Figure S1). More specifically, *E. bilineatus* (Figures 2 and 3) is known from the Rivers Maquiné and Três Forquilhas, both tributaries of the Tramandaí River system, whereas *Epactionotus itaimbezinho* (Figure 4) is endemic to the Mampituba River drainage and *Epactionotus gracilis* (Figure 5) to the Araranguá River drainage (Figure 1; Supporting Information Figure S1; Malabarba *et al*., 2013; Reis & Schaefer, 1998).

The genus was morphologically diagnosed from other Hypoptopomatinae (Reis & Schaefer, 1998; Schaefer, 1998) by several apomorphic features such as the presence of the posteriorly displaced dorsal fin, the absence of a fleshy flap in the dorsal portion of the first pelvic-fin ray in males and the presence of dentary and premaxillary accessory teeth. Recent phylogenetic studies contrast to some degree regarding the position of *Epactionotus* within Hypoptopomatinae (Chiachio *et al*., 2008; Gauger & Buckup, 2005; Roxo *et al*., 2019) but concur regarding its sister relationship with *Eurycheilichthys* (Cramer *et al*., 2007, 2011; Roxo *et al*., 2014).

Recent fieldwork in the Atlantic coastal drainages of southern Brazil has revealed new populations of *Epactionotus* north of their previous range limit in the Urussanga [also included in the FEOW (Freshwater Ecoregion of the World) 335], Tubarão, d'Una and Biguaçu River drainages, which are part of the Southeastern Mata Atlantica FEOW 331 (Figures 1 and 6–9; Supporting Information Figure S1). With regard to these new data, the status of *Epactionotus* species/populations was re-evaluated across these isolated drainages of southern Brazil, and a new species is described from the Biguaçu River drainage in Santa Catarina State.

## 2 | MATERIALS AND METHODS

### 2.1 | Ethical statement

In total, 106 individuals were sampled for morphology (Tables 1–4) and 28 specimens for molecular analyses (Supporting Information Table S1). Most fish specimens were previously available in

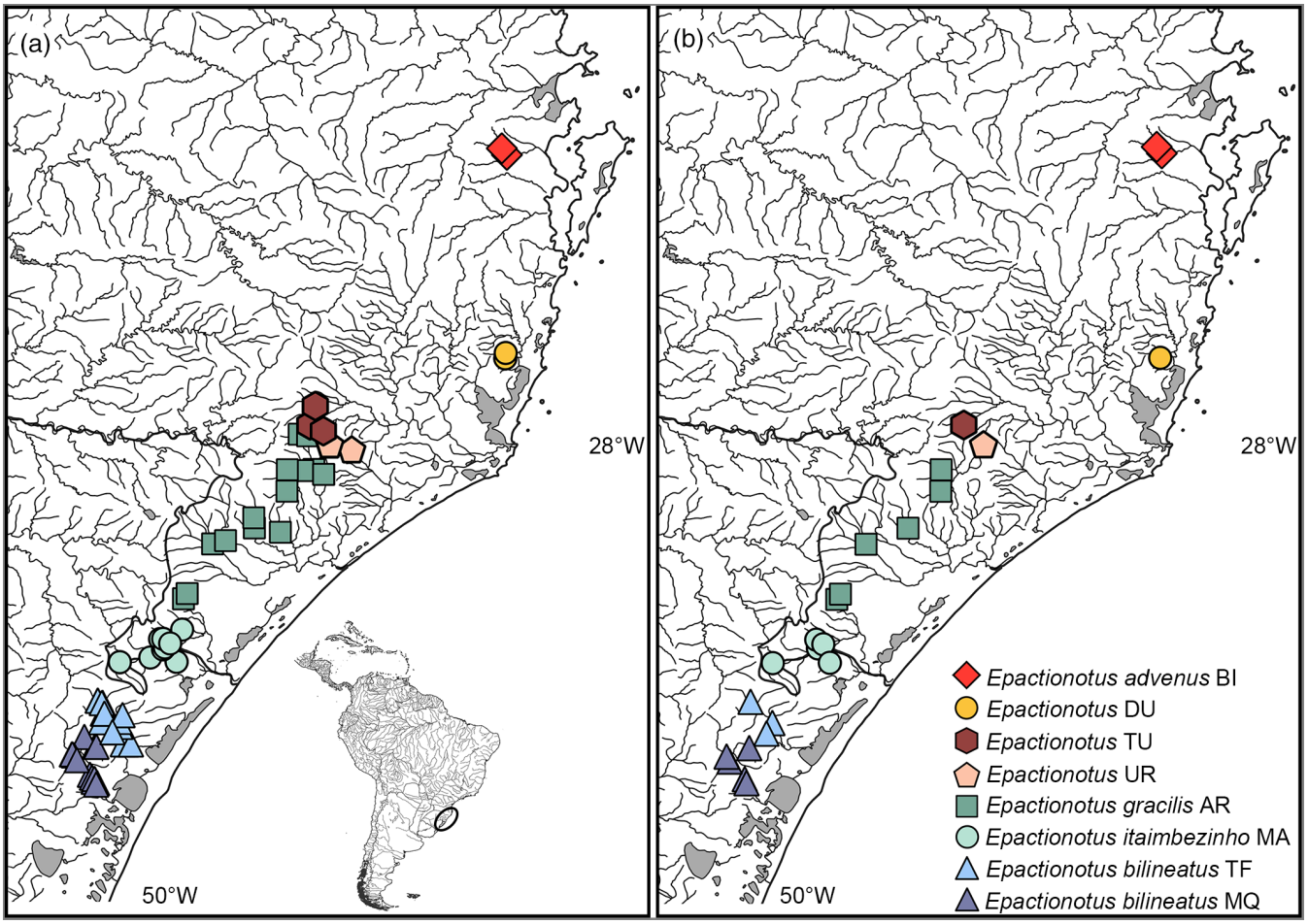


**FIGURE 1** Geographic distribution of the species/populations of *Epactionotus* based on (a) material examined and (b) sampling localities used for molecular analyses; following a south–north distribution. MQ: Maquiné; TF: Três Forquilhas; MA: Mampituba; AR: Araranguá; UR: Urussanga; TU: Tubarão; DU: d'Una; BI: Biguaçu

**FIGURE 2** *Epactionotus bilineatus* from Maquiné (MQ), MCP 19105, female, 30.6 mm standard length, Brazil, Rio Grande do Sul, Maquiné, Arroio do Ouro (29° 39′ 58″ S, 50° 10′ 59″ W)

**FIGURE 3** *Epactionotus bilineatus* from Três Forquilhas (TF), MCP 28978, male, 34.3 mm standard length, Brazil, Rio Grande do Sul, Três Forquilhas, Arroio Japonês, (*c.* 29° 32′ S, 50° 05′ W)

museum collections except for some (Supporting Information Table S1) that were specially collected for this study under collecting permit 10287 issued to R.E.R. and collection expedition permits 9318-1 and 9220-1 to T.P.C. from the Instituto Chico Mendes de Conservação da Biodiversidade of the Ministry of Environment.

**FIGURE 4** *Epactionotus itaimbezinho* from Mampituba (MA), MCP 23683, male, 34.9 mm standard length, Brazil, Santa Catarina, Morrinhos do Sul, Rio Mangue (29° 14′ 55″ S, 49° 55′ 30″ W)

**FIGURE 5** *Epactionotus gracilis* from Araranguá (AR), UFRGS 22945, male, 28.2 mm standard length, Brazil, Santa Catarina, Nova Veneza (28° 35′ 02.2″ S, 49° 32′ 31.2″ W)

## 2.2 | Morphological procedures and terminology

Individuals were diagnosed as *Epactionotus* based on the absence of an expanded fleshy flap on the dorsal surface of the first pelvic-fin ray of males, possession of accessory oral teeth and presence of two longitudinal light stripe markings on the dorsal surface of the head and trunk (Reis & Schaefer, 1998). Additional diagnostic osteological characters, such as the neural spine of the seventh vertebra contacting the unpaired predorsal plate anterior to the nuchal plate, dorsal-fin proximal radial contacting the eighth vertebra and absence of the

**FIGURE 6** *Epactionotus* sp. from Urussanga (UR), UFRGS 6212, female, 36.2 mm standard length, Brazil, Santa Catarina, Urussanga, Rio Lageado (28° 31′04.92″ S, 49° 19′ 10.07″ W)

**FIGURE 8** *Epactionotus* sp. from d'Una (DU), MZUEL 7528, female, 31.2 mm standard length, Brazil, Santa Catarina, Imarui, Rio d'Una (28° 10′ 48.8″ S, 48° 47′ 12.0″ W)

**FIGURE 7** *Epactionotus* sp. from Tubarão (TU), UFRGS 22941, male, 31.9 mm standard length, Brazil, Santa Catarina, Rio Bonito Alto (28° 25′ 48.3″ S, 49° 27′ 50.7″ W)

**FIGURE 9** *Epactionotus advenus*, sp. nov. from Biguaçu (BI), UFRGS 28220, holotype, female, 35.4 mm standard length, Brazil, Santa Catarina, Antônio Carlos, Rio Rachadel (27° 29′ 44″ S, 48° 46′ 57″ W)

connecting bone (Calegari *et al*., 2011; Delapieve *et al*., 2017; Martins *et al*., 2014; Reis & Schaefer, 1998; Rodriguez *et al*., 2015), were checked in cleared and double-stained specimens prepared according to a modification of the procedure described by Taylor and Van Dyke (1985).

Measurements were made on the left side of specimens point to point using digital callipers under a stereomicroscope. Morphometric measurements in tables and the species diagnosis were treated as percentages of standard length (SL), except for subunits of the head, which were treated as percentages of head length (HL). Counts of rays, vertebrae, teeth, and dermal plates were also conducted under the stereomicroscope, and the latter followed the serial homology and terminology proposed by Schaefer (1997). Measurements and counts followed the descriptions by Pereira *et al*. (2007) and include most of the modifications suggested by Calegari *et al*. (2011, 2014) and Lippert *et al*. (2014). Vertebral counts include all vertebral centra, including the five centra that comprise the Weberian apparatus, and the caudal complex centrum (PU1 + U1) counted as a single element.

Morphometric data, except the number of vertebrae, were statistically analysed according to populations and species of *Epactionotus* by drainage. Counts were analysed using ANOVA, aiming to compare means across groups. Tukey's test was used to determine which counts are significantly different between groups

**TABLE 1** Descriptive morphometrics of species/populations of *Epactionotus* by drainage

| | *Epactionotus bilineatus* (MQ) | | | | *E. bilineatus* (TF) | | | | *Epactionotus itaimbezinho* (MA) | | | | *Epactionotus gracilis* (AR) | | | | *Epactionotus* (UR) | | | |
|---|---|---|---|---|---|---|---|---|---|---|---|---|---|---|---|---|---|---|---|---|
| | *N* = 13 | | | | *N* = 12 | | | | *N* = 12 | | | | *N* = 13 | | | | *N* = 15 | | | |
| | Low | High | Mean | S.D. | Low | High | Mean | S.D. | Low | High | Mean | S.D. | Low | High | Mean | S.D. | Low | High | Mean | S.D. |
| Standard length (mm) | 32.7 | 36.0 | 34.3 | 1.0 | 32.6 | 35.6 | 33.6 | 1.0 | 33.4 | 38.5 | 36.5 | 1.9 | 30.3 | 37.6 | 34.0 | 2.3 | 28.9 | 36.4 | 32.4 | 2.2 |
| *Percentage of SL* | | | | | | | | | | | | | | | | | | | | |
| Head length | 32.3 | 35.0 | 33.4 | 0.9 | 32.0 | 34.8 | 33.4 | 0.7 | 32.6 | 34.9 | 33.7 | 0.8 | 30.9 | 34.4 | 32.9 | 0.9 | 30.7 | 35.4 | 32.7 | 1.1 |
| Predorsal length | 44.9 | 48.9 | 46.9 | 1.2 | 46.1 | 48.3 | 47.1 | 0.8 | 46.0 | 48.8 | 47.7 | 0.9 | 45.3 | 49.8 | 47.9 | 1.4 | 44.1 | 49.7 | 47.4 | 1.3 |
| Postdorsal length | 41.3 | 47.2 | 43.9 | 1.6 | 41.6 | 43.9 | 43.2 | 0.8 | 42.5 | 45.0 | 43.2 | 0.7 | 39.9 | 45.5 | 43.3 | 2.0 | 41.0 | 46.8 | 45.3 | 1.4 |
| Prepectoral length | 24.6 | 26.8 | 25.7 | 0.6 | 24.5 | 27.0 | 25.8 | 0.8 | 24.2 | 26.7 | 25.7 | 0.7 | 24.2 | 27.1 | 25.4 | 0.8 | 24.5 | 27.1 | 25.6 | 0.8 |
| Prepelvic length | 40.6 | 43.2 | 42.1 | 0.8 | 40.8 | 43.6 | 42.1 | 1.0 | 40.4 | 43.8 | 42.4 | 1.0 | 40.4 | 43.6 | 41.6 | 0.9 | 39.0 | 44.4 | 41.8 | 1.2 |
| Pre-anal length | 59.8 | 63.4 | 62.2 | 1.0 | 61.3 | 63.4 | 62.2 | 0.7 | 60.6 | 64.4 | 62.5 | 1.0 | 59.8 | 64.3 | 61.8 | 1.5 | 59.4 | 63.3 | 61.3 | 1.1 |
| Cleithral width | 23.6 | 26.1 | 24.6 | 0.8 | 23.1 | 25.0 | 24.1 | 0.6 | 22.2 | 23.8 | 22.9 | 0.5 | 20.1 | 23.3 | 21.7 | 0.9 | 20.6 | 22.8 | 21.8 | 0.7 |
| Pectoral–pelvic fin distance | 16.7 | 19.3 | 18.0 | 0.9 | 16.1 | 18.8 | 17.3 | 0.8 | 15.3 | 19.1 | 17.6 | 1.1 | 15.2 | 18.1 | 16.8 | 0.8 | 16.1 | 19.6 | 17.8 | 0.9 |
| Pelvic–anal fin distance | 21.0 | 24.3 | 22.6 | 0.8 | 20.8 | 22.9 | 21.7 | 0.6 | 20.4 | 23.3 | 21.9 | 0.8 | 19.6 | 23.9 | 21.9 | 1.2 | 19.3 | 23.0 | 21.7 | 0.9 |
| Dorsal-fin spine length | 20.3 | 23.6 | 21.7 | 0.9 | 19.2 | 21.9 | 20.8 | 0.9 | 18.4 | 22.6 | 20.9 | 1.3 | 18.3 | 22.1 | 20.3 | 1.1 | 17.0 | 21.9 | 19.8 | 1.4 |
| Dorsal-fin base length | 10.6 | 12.8 | 11.9 | 0.7 | 11.1 | 13.0 | 12.0 | 0.7 | 11.3 | 12.6 | 12.0 | 0.4 | 9.9 | 12.8 | 11.2 | 0.8 | 9.1 | 11.1 | 10.2 | 0.5 |
| Pectoral-fin spine length | 20.2 | 22.7 | 21.5 | 0.8 | 20.5 | 23.1 | 21.9 | 0.8 | 19.1 | 21.6 | 20.7 | 0.8 | 18.0 | 22.4 | 20.9 | 1.5 | 17.4 | 21.5 | 19.8 | 1.2 |
| Pectoral-fin length | 22.6 | 26.1 | 24.0 | 0.8 | 22.3 | 24.7 | 24.0 | 0.7 | 20.9 | 23.9 | 22.9 | 0.8 | 20.5 | 24.5 | 22.9 | 1.4 | 19.8 | 23.4 | 21.8 | 1.3 |
| First pelvic-fin unbranched ray length | 16.3 | 19.4 | 17.3 | 0.8 | 16.6 | 17.6 | 17.1 | 0.3 | 15.0 | 16.9 | 16.0 | 0.6 | 14.7 | 18.4 | 16.3 | 1.0 | 13.8 | 16.7 | 15.5 | 0.8 |
| First pelvic-fin unbranched ray width | 6.2 | 8.9 | 7.3 | 0.8 | 6.9 | 9.5 | 7.7 | 0.7 | 6.3 | 8.9 | 7.8 | 0.8 | 6.4 | 8.7 | 7.4 | 0.7 | 5.3 | 9.4 | 6.8 | 1.0 |
| First anal-fin unbranched ray length | 13.0 | 15.7 | 14.5 | 0.9 | 14.0 | 15.7 | 15.1 | 0.5 | 13.1 | 16.9 | 15.0 | 1.0 | 13.1 | 15.9 | 14.7 | 0.9 | 12.0 | 15.5 | 14.0 | 1.0 |
| Caudal-peduncle length | 37.2 | 40.5 | 38.7 | 1.0 | 37.0 | 40.0 | 38.3 | 0.8 | 36.1 | 38.5 | 37.3 | 0.7 | 36.9 | 40.3 | 38.8 | 1.1 | 37.3 | 41.8 | 40.0 | 1.2 |
| Caudal-peduncle depth | 9.2 | 10.7 | 10.0 | 0.4 | 9.8 | 10.8 | 10.3 | 0.3 | 9.9 | 11.2 | 10.5 | 0.5 | 9.8 | 10.9 | 10.5 | 0.4 | 8.8 | 10.4 | 9.5 | 0.5 |
| Caudal-peduncle width | 5.8 | 7.2 | 6.5 | 0.5 | 4.9 | 5.8 | 5.5 | 0.3 | 4.7 | 5.8 | 5.3 | 0.3 | 4.9 | 5.9 | 5.4 | 0.3 | 5.1 | 8.2 | 6.3 | 0.9 |
| Body depth at dorsal-fin origin | 14.1 | 18.3 | 15.5 | 1.2 | 13.0 | 15.5 | 14.4 | 0.8 | 13.3 | 16.4 | 15.3 | 0.9 | 12.1 | 16.5 | 14.4 | 1.2 | 13.4 | 16.0 | 14.3 | 0.8 |
| Body width at dorsal-fin origin | 18.6 | 26.6 | 21.3 | 2.4 | 17.5 | 21.2 | 19.1 | 1.0 | 18.5 | 21.5 | 19.8 | 1.0 | 15.4 | 22.6 | 18.4 | 2.2 | 17.2 | 22.8 | 19.9 | 2.0 |
| *Percentage of HL* | | | | | | | | | | | | | | | | | | | | |
| Head depth | 39.7 | 44.7 | 41.9 | 1.5 | 40.1 | 44.6 | 42.7 | 1.1 | 39.8 | 43.0 | 41.7 | 1.0 | 39.0 | 45.8 | 43.0 | 2.3 | 37.0 | 42.8 | 40.3 | 1.5 |
| Head width | 70.2 | 77.2 | 73.8 | 2.2 | 70.7 | 74.9 | 72.2 | 1.4 | 64.1 | 69.4 | 66.5 | 1.2 | 61.9 | 69.8 | 66.4 | 2.6 | 63.5 | 69.2 | 66.1 | 2.0 |
| Snout length | 51.7 | 56.1 | 53.9 | 1.4 | 51.3 | 55.0 | 53.6 | 1.1 | 51.3 | 54.8 | 53.0 | 1.2 | 50.3 | 55.6 | 53.3 | 1.5 | 49.6 | 52.9 | 51.1 | 1.0 |
| Orbital diameter | 13.2 | 15.2 | 14.2 | 0.7 | 14.5 | 15.9 | 15.2 | 0.5 | 12.7 | 14.9 | 13.9 | 0.7 | 13.5 | 15.9 | 14.9 | 0.7 | 12.4 | 16.3 | 14.1 | 1.0 |
| Snout–opercle distance | 76.2 | 81.7 | 78.4 | 1.7 | 77.2 | 82.9 | 79.9 | 1.7 | 76.2 | 80.7 | 77.8 | 1.5 | 74.9 | 81.3 | 79.0 | 1.5 | 74.2 | 80.8 | 78.1 | 2.0 |

**TABLE 1** (Continued)

| | *Epactionotus bilineatus* (MQ) | | | *E. bilineatus* (TF) | | | *Epactionotus itaimbezinho* (MA) | | | *Epactionotus gracilis* (AR) | | | *Epactionotus* (UR) | | |
|---|---|---|---|---|---|---|---|---|---|---|---|---|---|---|---|
| | N = 13 | | | N = 12 | | | N = 12 | | | N = 13 | | | N = 15 | | |
| | Low | High | Mean | s.d. | Low | High | Mean | s.d. | Low | High | Mean | s.d. | Low | High | Mean | s.d. | Low | High | Mean | s.d. |
| Interorbital distance | 38.4 | 42.3 | 39.6 | 1.1 | 38.4 | 40.9 | 39.5 | 0.8 | 36.6 | 40.5 | 38.9 | 1.3 | 37.0 | 41.2 | 39.4 | 1.1 | 35.7 | 42.6 | 39.2 | 2.6 |
| Internareal width | 11.1 | 14.2 | 13.1 | 0.9 | 11.9 | 15.0 | 13.5 | 0.8 | 11.6 | 14.2 | 12.8 | 0.8 | 10.9 | 14.2 | 12.2 | 1.1 | 11.2 | 14.3 | 12.6 | 1.0 |
| Nares diameter | 9.1 | 11.9 | 10.2 | 0.8 | 8.4 | 11.2 | 10.0 | 0.8 | 8.0 | 10.6 | 9.4 | 0.7 | 9.0 | 12.5 | 10.5 | 1.0 | 9.2 | 11.3 | 10.3 | 0.6 |
| Prenasal length | 33.1 | 36.6 | 35.0 | 1.0 | 34.6 | 36.7 | 35.7 | 0.6 | 34.4 | 37.3 | 36.0 | 1.0 | 33.0 | 37.9 | 35.1 | 1.6 | 30.9 | 34.9 | 32.9 | 1.0 |
| Suborbital depth | 15.1 | 18.0 | 16.7 | 1.0 | 15.2 | 20.3 | 17.8 | 1.2 | 15.7 | 19.1 | 17.6 | 0.9 | 15.0 | 19.4 | 17.4 | 1.4 | 13.3 | 16.5 | 14.9 | 1.0 |

*Note*: Following a south–north distribution (part). Values are given as percentage of standard length (SL) or head length (HL). AR: Araranguá; MA: Mampituba; MQ: Maquiné; TF: Três Forquilhas; UR: Urussanga.

using Past v. 3.12 (Paleontological Statistics, Hammer *et al*., 2001). Based on Tukey's pair-wise results, box plots were also created using Past. Even though the number of medium abdominal plates did not show a statistically significant variation (see the "Results" section), it was considered a diagnostic character to distinguish species by the method of Reis and Schaefer (1998). Therefore, the aim was to visualize the distribution of this meristic feature in the new populations, and a box plot was also built for this character.

Before statistically analysing morphometric data, the VARSEDIG algorithm (Chuctaya *et al*., 2018; Faustino-Fuster *et al*., 2019; Guisande *et al*., 2016; Leigh & Bryant, 2015) was used in Rstudio version 3.6.1 (RStudio Team, 2020) to identify measurements that could be significantly associated with sexual dimorphism in *Epactionotus*. A linear regression was then conducted to describe the morphometric character found to discriminate males and females. After excluding the measurement associated with sexual dimorphism (*i.e*., width of pelvic-fin unbranched ray), statistical analyses were conducted, and all remaining morphometric variables were standardized, according to Aitchison (1982) log-ratio transformation to adjust for size variation. The Aitchison-transformed data were then used in a permutational multivariate analysis of variance (PERMANOVA) in Past to compare the different groups and test if centroids and dispersion are equivalent for all groups (Anderson, 2001). The same data set was used in both PCA and linear discriminant analysis (LDA), also performed in Past, to, respectively, search for general patterns of variation among specimens (Leal & Sant'Anna, 2006) and assess between-group patterns of body shape variation.

The Unified Species Concept (de Queiroz, 2007) was used in the present study, in which species are considered as independently evolving metapopulation lineages and different lines of evidence are operational criteria, being relevant to assessing lineage separation. In addition, the Concept understands that the presence of any property (if appropriately interpreted) can be used as evidence for the existence of a species, and the presence of more lines of evidence was associated with a higher degree of support.

Institutional abbreviations are those listed at https://asih.org/sites/default/files/2019-04/Sabaj_2019_ASIH_Symbolic_Codes_v7.1.pdf (Sabaj, 2019), except for UNICTIO, which stands for Coleçãode Referência do Laboratório de Ictiologia da Universidade do Vale do Rio dos Sinos (UNISINOS).

## 2.3 | Distribution map

The distribution map was created using QGIS software (v. 3.8 - QGIS Development Team, 2020), with shape and raster files from the databases of IBGE (Instituto Brasileiro de Geografia e Estatística: http://mapas.ibge.gov.br/bases-e-referenciais) and Agência Nacional de Águas: http://www.snirh.gov.br/hidroweb and following the tutorial provided by Calegari *et al*. (2016). Species distribution data include all

**TABLE 2** Descriptive morphometrics of species/populations of *Epactionotus* by drainage following a south–north distribution (part)

| | *Epactionotus* (TU) | | | | *Epactionotus* (DU) | | | | *Epactionotus advenus* (BI) | | | | |
|---|---|---|---|---|---|---|---|---|---|---|---|---|---|
| | *N* = 6 | | | | *N* = 12 | | | | *N* = 23 | | | | |
| | Low | High | Mean | S.D. | Low | High | Mean | S.D. | Hol | Low | High | Mean | S.D. |
| Standard length (mm) | 28.3 | 35.8 | 31.9 | 2.5 | 27.9 | 34.0 | 31.0 | 1.9 | 35.4 | 32.7 | 39.0 | 36.6 | 1.6 |
| *Percentage of SL* | | | | | | | | | | | | | |
| Head length | 31.8 | 35.0 | 33.4 | 1.2 | 32.4 | 36.4 | 34.4 | 1.2 | 33.3 | 30.8 | 34.8 | 32.4 | 0.9 |
| Predorsal length | 46.8 | 49.7 | 48.0 | 1.1 | 48.1 | 52.4 | 49.6 | 1.3 | 48.1 | 46.0 | 49.9 | 47.7 | 0.9 |
| Postdorsal length | 44.9 | 46.6 | 45.4 | 0.7 | 42.6 | 47.5 | 44.4 | 1.6 | 44.2 | 41.4 | 47.1 | 44.2 | 1.5 |
| Prepectoral length | 25.1 | 28.7 | 26.3 | 1.4 | 25.1 | 28.2 | 26.8 | 1.0 | 25.9 | 23.6 | 26.5 | 24.8 | 0.8 |
| Prepelvic length | 41.7 | 44.5 | 42.5 | 1.0 | 39.3 | 42.6 | 40.6 | 0.9 | 43.2 | 38.8 | 43.2 | 40.9 | 1.1 |
| Pre-anal length | 60.4 | 65.5 | 62.1 | 1.8 | 59.3 | 62.1 | 60.8 | 0.9 | 63.1 | 58.8 | 63.1 | 60.8 | 1.2 |
| Cleithral width | 22.1 | 24.3 | 23.1 | 0.9 | 20.0 | 22.3 | 21.0 | 0.7 | 20.8 | 19.0 | 20.8 | 20.2 | 0.5 |
| Pectoral–pelvic fin distance | 15.7 | 18.7 | 17.7 | 1.2 | 13.8 | 16.6 | 15.3 | 0.7 | 17.9 | 15.0 | 18.5 | 16.7 | 0.9 |
| Pelvic–anal fin distance | 20.8 | 24.1 | 22.4 | 1.3 | 20.6 | 23.1 | 21.5 | 0.7 | 21.9 | 20.0 | 23.4 | 21.6 | 0.9 |
| Dorsal-fin spine length | 19.2 | 22.8 | 21.1 | 1.3 | 17.0 | 20.2 | 19.0 | 0.8 | 19.3 | 17.3 | 20.0 | 18.6 | 0.9 |
| Dorsal-fin base length | 9.6 | 14.1 | 11.4 | 1.7 | 10.2 | 11.6 | 10.8 | 0.5 | 11.8 | 9.6 | 12.3 | 11.1 | 0.8 |
| Pectoral-fin spine length | 19.3 | 20.7 | 20.2 | 0.5 | 17.9 | 22.3 | 19.2 | 1.4 | 17.2 | 15.5 | 18.8 | 17.0 | 0.9 |
| Pectoral-fin length | 22.3 | 23.5 | 23.1 | 0.5 | 18.0 | 22.6 | 20.9 | 1.2 | 20.9 | 19.0 | 22.3 | 20.4 | 0.8 |
| First pelvic-fin unbranched ray length | 15.3 | 16.5 | 15.8 | 0.4 | 15.2 | 17.6 | 16.4 | 0.7 | 16.5 | 13.6 | 16.5 | 15.1 | 0.8 |
| First pelvic-fin unbranched ray width | 6.1 | 9.3 | 7.9 | 1.1 | 4.2 | 7.8 | 6.1 | 0.9 | 6.6 | 6.6 | 9.9 | 8.0 | 1.0 |
| First anal-fin unbranched ray length | 13.5 | 15.7 | 14.6 | 0.8 | 12.8 | 14.9 | 13.8 | 0.7 | 14.2 | 11.2 | 14.6 | 12.9 | 1.1 |
| Caudal-peduncle length | 37.6 | 41.5 | 39.3 | 1.3 | 38.9 | 40.8 | 39.7 | 0.6 | 40.6 | 38.1 | 41.6 | 39.8 | 1.1 |
| Caudal-peduncle depth | 9.3 | 10.7 | 10.0 | 0.6 | 8.4 | 9.4 | 9.0 | 0.3 | 9.1 | 7.7 | 9.3 | 8.7 | 0.4 |
| Caudal-peduncle width | 5.2 | 6.8 | 6.0 | 0.6 | 4.1 | 6.0 | 4.7 | 0.6 | 5.5 | 4.1 | 5.8 | 4.9 | 0.4 |
| Body depth at dorsal-fin origin | 12.3 | 17.0 | 15.1 | 2.1 | 11.7 | 13.8 | 13.0 | 0.5 | 14.2 | 11.1 | 14.2 | 12.8 | 1.0 |
| Body width at dorsal-fin origin | 17.2 | 24.2 | 21.0 | 3.0 | 16.6 | 19.2 | 17.7 | 0.9 | 18.6 | 14.9 | 20.2 | 17.3 | 1.3 |
| *Percentage of HL* | | | | | | | | | | | | | |
| Head depth | 40.5 | 42.6 | 41.4 | 0.8 | 35.6 | 38.8 | 37.5 | 1.1 | 40.2 | 37.0 | 43.2 | 39.2 | 1.6 |
| Head width | 67.1 | 71.6 | 68.9 | 1.8 | 56.6 | 63.6 | 60.4 | 2.3 | 63.6 | 59.5 | 66.6 | 63.0 | 1.6 |
| Snout length | 51.4 | 56.0 | 53.3 | 1.8 | 52.4 | 55.0 | 53.8 | 0.8 | 51.9 | 51.1 | 55.4 | 52.9 | 1.1 |
| Orbital diameter | 14.7 | 16.1 | 15.6 | 0.5 | 12.8 | 15.1 | 13.6 | 0.8 | 14.6 | 12.8 | 15.5 | 14.4 | 0.8 |
| Snout–opercle distance | 78.2 | 82.3 | 80.3 | 1.5 | 76.2 | 81.4 | 78.6 | 1.6 | 77.6 | 75.6 | 81.9 | 78.1 | 1.5 |
| Interorbital distance | 39.1 | 41.2 | 40.4 | 0.7 | 33.3 | 37.4 | 35.5 | 1.3 | 37.0 | 34.5 | 38.6 | 37.1 | 0.9 |
| Internareal width | 11.1 | 13.7 | 12.9 | 1.0 | 9.3 | 12.7 | 11.5 | 1.0 | 12.8 | 11.3 | 13.9 | 12.5 | 0.8 |
| Nares diameter | 7.9 | 12.3 | 10.5 | 1.5 | 8.9 | 11.8 | 10.1 | 0.8 | 8.9 | 8.4 | 10.6 | 9.6 | 0.6 |
| Prenasal length | 31.6 | 36.2 | 34.3 | 1.6 | 33.8 | 37.9 | 36.0 | 1.3 | 35.1 | 33.5 | 38.0 | 35.3 | 1.3 |
| Suborbital depth | 15.4 | 17.3 | 16.5 | 0.8 | 13.1 | 16.5 | 14.8 | 1.1 | 16.1 | 13.9 | 18.2 | 16.1 | 1.3 |

*Note:* Values are given as percentage of standard length (SL) or head length (HL). BI: Biguaçu; DU: d'Una; Hol: holotype; TU: Tubarão.

records from Reis and Schaefer (1998) and available material in the collections of MCN, MCP, MZUEL, UFRGS and UNICTIO.

## 2.4 | Molecular data and alignment

Tissue sample vouchers include material deposited in the collections of MCP, UFRGS and UNICTIO. Muscle samples were removed from specimens, preserved in 99.8% ethanol and stored in freezers at −20°C. From the ethanol-preserved samples, total genomic DNA was extracted using the DNeasy Blood and Tissue extraction kits (Qiagen, Valencia, CA, USA) following the manufacturer's protocol for animal tissues. DNA extractions from 23 individuals of *Epactionotus* (Supporting Information Table S1) were stored at −20°C, and partial sequences of the mitochondrial cytochrome c oxidase subunit I (COI) gene were amplified using the primers COI L6252-Asn (5′-AAG GCG

**TABLE 3** Descriptive counts of species/populations of *Epactionotus* by drainage following a south–north distribution (part)

| | *Epactionotus bilineatus* (MQ) | | | | *E. bilineatus* (TF) | | | | *Epactionotus itaimbezinho* (MA) | | | | *Epactionotus gracilis* (AR) | | | | *Epactionotus* (UR) | | | |
|---|---|---|---|---|---|---|---|---|---|---|---|---|---|---|---|---|---|---|---|---|
| | *N* = 13 | | | | *N* = 12 | | | | *N* = 12 | | | | *N* = 13 | | | | *N* = 15 | | | |
| Counts | Low | High | Mean | S.D. | Low | High | Mean | S.D. | Low | High | Mean | S.D. | Low | High | Mean | S.D. | Low | High | Mean | S.D. |
| Right premaxillary teeth | 17 | 21 | 18.7 | 1.5 | 16.0 | 21.0 | 18.2 | 1.6 | 16.0 | 23.0 | 19.3 | 2.4 | 16.0 | 23.0 | 18.5 | 2.0 | 15.0 | 22.0 | 18.3 | 1.6 |
| Left premaxillary teeth | 17 | 21 | 19.2 | 1.4 | 16.0 | 21.0 | 18.8 | 1.5 | 17.0 | 22.0 | 19.2 | 1.9 | 16.0 | 23.0 | 18.2 | 1.9 | 16.0 | 21.0 | 18.9 | 1.6 |
| Right dentary teeth | 17 | 21 | 18.9 | 1.5 | 16.0 | 20.0 | 18.3 | 1.5 | 15.0 | 21.0 | 18.5 | 1.7 | 15.0 | 20.0 | 17.2 | 1.5 | 14.0 | 19.0 | 16.8 | 1.6 |
| Left dentary teeth | 17 | 21 | 18.8 | 1.2 | 15.0 | 21.0 | 18.0 | 1.6 | 16.0 | 21.0 | 18.1 | 1.5 | 15.0 | 20.0 | 16.9 | 1.8 | 13.0 | 19.0 | 16.4 | 1.6 |
| Plates in median lateral series | 25 | 27 | 25.8 | 0.6 | 25.0 | 28.0 | 26.4 | 0.9 | 25.0 | 28.0 | 26.7 | 0.9 | 26.0 | 27.0 | 26.7 | 0.5 | 25.0 | 28.0 | 26.5 | 0.7 |
| Plates in mid-dorsal series | 21 | 24 | 22.7 | 0.9 | 22.0 | 24.0 | 23.1 | 0.5 | 22.0 | 25.0 | 23.5 | 0.8 | 22.0 | 24.0 | 23.4 | 0.8 | 23.0 | 25.0 | 24.0 | 0.8 |
| Plates in dorsal series | 23 | 24 | 23.1 | 0.3 | 22.0 | 23.0 | 22.3 | 0.5 | 22.0 | 24.0 | 23.0 | 0.4 | 22.0 | 23.0 | 22.6 | 0.5 | 22.0 | 24.0 | 22.8 | 0.6 |
| Plates in mid-ventral series | 22 | 24 | 22.9 | 0.8 | 23.0 | 24.0 | 23.3 | 0.5 | 23.0 | 25.0 | 23.9 | 0.8 | 22.0 | 27.0 | 24.1 | 1.4 | 22.0 | 25.0 | 23.8 | 0.8 |
| Plates in ventral series | 20 | 24 | 22.7 | 1.3 | 22.0 | 24.0 | 23.1 | 0.8 | 22.0 | 24.0 | 23.4 | 0.7 | 20.0 | 27.0 | 23.1 | 2.0 | 22.0 | 25.0 | 23.7 | 1.0 |
| Plates between anal and caudal fin series | 12 | 13 | 12.3 | 0.5 | 11.0 | 14.0 | 12.3 | 0.8 | 12.0 | 13.0 | 12.7 | 0.5 | 12.0 | 13.0 | 12.8 | 0.4 | 12.0 | 14.0 | 12.9 | 0.5 |
| Plates at dorsal-fin base | 5 | 6 | 5.5 | 0.5 | 5.0 | 6.0 | 5.4 | 0.5 | 5.0 | 6.0 | 5.3 | 0.5 | 5.0 | 6.0 | 5.1 | 0.3 | 4.0 | 5.0 | 4.9 | 0.3 |
| Plates at anal-fin base | 3 | 4 | 3.1 | 0.3 | 3.0 | 4.0 | 3.3 | 0.5 | 3.0 | 4.0 | 3.2 | 0.4 | 3.0 | 3.0 | 3.0 | 0.0 | 2.0 | 3.0 | 2.9 | 0.3 |
| Unpaired predorsal plates | 0 | 1 | 0.5 | 0.5 | 0.0 | 1.0 | 0.6 | 0.5 | 0.0 | 3.0 | 1.6 | 0.8 | 1.0 | 3.0 | 1.5 | 0.7 | 1.0 | 2.0 | 1.3 | 0.5 |
| Predorsal plates | 3 | 4 | 3.8 | 0.4 | 4.0 | 4.0 | 4.0 | 0.0 | 3.0 | 4.0 | 3.9 | 0.3 | 4.0 | 4.0 | 4.0 | 0.0 | 4.0 | 4.0 | 4.0 | 0.0 |
| Right abdominal plates | 0 | 6 | 2.5 | 1.7 | 1.0 | 7.0 | 3.8 | 1.9 | 3.0 | 6.0 | 4.1 | 0.8 | 2.0 | 6.0 | 3.8 | 1.4 | 2.0 | 7.0 | 4.7 | 1.4 |
| Left abdominal plates | 1 | 5 | 2.5 | 1.4 | 1.0 | 7.0 | 4.0 | 1.7 | 3.0 | 7.0 | 4.3 | 1.4 | 2.0 | 5.0 | 3.5 | 1.1 | 3.0 | 7.0 | 4.5 | 1.4 |
| Medium abdominal plates | 0 | 1 | 0.4 | 0.5 | 0.0 | 20.0 | 4.8 | 6.0 | 0.0 | 25.0 | 7.8 | 8.2 | 0.0 | 16.0 | 5.6 | 4.8 | 0.0 | 40.0 | 8.5 | 10.3 |
| Pectoral-fin rays | 6 | 6 | 6.0 | 0.0 | 6.0 | 6.0 | 6.0 | 0.0 | 6.0 | 6.0 | 6.0 | 0.0 | 6.0 | 6.0 | 6.0 | 0.0 | 6.0 | 6.0 | 6.0 | 0.0 |
| Dorsal-fin rays | 7 | 7 | 7.0 | 0.0 | 7.0 | 7.0 | 7.0 | 0.0 | 7.0 | 7.0 | 7.0 | 0.0 | 7.0 | 7.0 | 7.0 | 0.0 | 7.0 | 7.0 | 7.0 | 0.0 |
| Pelvic-fin rays | 5 | 5 | 5.0 | 0.0 | 5.0 | 5.0 | 5.0 | 0.0 | 5.0 | 5.0 | 5.0 | 0.0 | 5.0 | 5.0 | 5.0 | 0.0 | 5.0 | 5.0 | 5.0 | 0.0 |
| Anal-fin rays | 5 | 5 | 5.0 | 0.0 | 5.0 | 5.0 | 5.0 | 0.0 | 5.0 | 5.0 | 5.0 | 0.0 | 5.0 | 5.0 | 5.0 | 0.0 | 5.0 | 5.0 | 5.0 | 0.0 |
| Caudal-fin rays | 14 | 14 | 14.0 | 0.0 | 14.0 | 14.0 | 14.0 | 0.0 | 13.0 | 14.0 | 13.9 | 0.3 | 13.0 | 14.0 | 13.8 | 0.4 | 13.0 | 14.0 | 13.9 | 0.4 |

*Note:* AR: Araranguá; MA: Mampituba; MQ: Maquiné; TF: Três Forquilhas; UR: Urussanga.

**TABLE 4** Descriptive counts of species/populations of *Epactionotus* by drainage following a south–north distribution (part)

| | *Epactionotus* (TU) | | | | *Epactionotus* (DU) | | | | *Epactionotus advenus* (BI) | | | | |
|---|---|---|---|---|---|---|---|---|---|---|---|---|---|
| | *N* = 6 | | | | *N* = 12 | | | | *N* = 23 | | | | |
| Counts | Low | High | Mean | S.D. | Low | High | Mean | S.D. | Hol | Low | High | Mean | S.D. |
| Right premaxillary teeth | 16.0 | 21.0 | 18.0 | 2.0 | 19.0 | 25.0 | 21.5 | 1.4 | 19.0 | 15.0 | 21.0 | 17.6 | 1.6 |
| Left premaxillary teeth | 16.0 | 19.0 | 17.5 | 1.2 | 19.0 | 26.0 | 21.0 | 1.8 | 19.0 | 15.0 | 20.0 | 17.7 | 1.2 |
| Right dentary teeth | 15.0 | 18.0 | 16.3 | 1.0 | 16.0 | 20.0 | 18.4 | 1.3 | 17.0 | 14.0 | 18.0 | 16.0 | 1.1 |
| Left dentary teeth | 15.0 | 18.0 | 16.3 | 1.0 | 15.0 | 20.0 | 18.0 | 1.6 | 17.0 | 14.0 | 19.0 | 16.3 | 1.3 |
| Plates in median lateral series | 26.0 | 27.0 | 26.5 | 0.5 | 25.0 | 27.0 | 25.8 | 0.6 | 28.0 | 26.0 | 29.0 | 27.1 | 0.8 |
| Plates in mid-dorsal series | 24.0 | 24.0 | 24.0 | 0.0 | 21.0 | 23.0 | 22.5 | 0.7 | 24.0 | 23.0 | 26.0 | 24.3 | 0.8 |
| Plates in dorsal series | 22.0 | 23.0 | 22.8 | 0.4 | 22.0 | 23.0 | 22.5 | 0.5 | 23.0 | 23.0 | 24.0 | 23.3 | 0.5 |
| Plates in mid-ventral series | 24.0 | 25.0 | 24.2 | 0.4 | 22.0 | 23.0 | 22.4 | 0.5 | 26.0 | 22.0 | 26.0 | 24.5 | 1.1 |
| Plates in ventral series | 24.0 | 25.0 | 24.2 | 0.4 | 21.0 | 24.0 | 22.4 | 0.8 | 26.0 | 23.0 | 26.0 | 25.0 | 0.9 |
| Plates between anal and caudal fin series | 13.0 | 13.0 | 13.0 | 0.0 | 12.0 | 14.0 | 12.7 | 0.7 | 14.0 | 12.0 | 14.0 | 13.1 | 0.5 |
| Plates at dorsal-fin base | 5.0 | 5.0 | 5.0 | 0.0 | 5.0 | 5.0 | 5.0 | 0.0 | 5.0 | 5.0 | 6.0 | 5.0 | 0.2 |
| Plates at anal-fin base | 3.0 | 3.0 | 3.0 | 0.0 | 3.0 | 3.0 | 3.0 | 0.0 | 3.0 | 2.0 | 3.0 | 3.0 | 0.2 |
| Unpaired predorsal plates | 0.0 | 2.0 | 1.2 | 0.8 | 0.0 | 2.0 | 1.0 | 0.4 | 3.0 | 1.0 | 3.0 | 2.0 | 0.6 |
| Predorsal plates | 4.0 | 5.0 | 4.2 | 0.4 | 4.0 | 4.0 | 4.0 | 0.0 | 4.0 | 4.0 | 5.0 | 4.1 | 0.3 |
| Right abdominal plates | 2.0 | 7.0 | 4.0 | 1.7 | 1.0 | 6.0 | 3.2 | 1.6 | 1.0 | 0.0 | 4.0 | 1.0 | 1.0 |
| Left abdominal plates | 2.0 | 7.0 | 4.2 | 1.6 | 1.0 | 5.0 | 3.6 | 1.2 | 1.0 | 0.0 | 4.0 | 0.9 | 0.9 |
| Medium abdominal plates | 0.0 | 12.0 | 5.2 | 4.2 | 0.0 | 13.0 | 1.3 | 3.7 | 0.0 | 0.0 | 0.0 | 0.0 | 0.0 |
| Pectoral-fin rays | 6.0 | 6.0 | 6.0 | 0.0 | 6.0 | 6.0 | 6.0 | 0.0 | 6.0 | 6.0 | 6.0 | 6.0 | 0.0 |
| Dorsal-fin rays | 7.0 | 7.0 | 7.0 | 0.0 | 6.0 | 7.0 | 6.9 | 0.3 | 7.0 | 7.0 | 8.0 | 7.0 | 0.2 |
| Pelvic-fin rays | 5.0 | 5.0 | 5.0 | 0.0 | 5.0 | 5.0 | 5.0 | 0.0 | 5.0 | 5.0 | 5.0 | 5.0 | 0.0 |
| Anal-fin rays | 5.0 | 5.0 | 5.0 | 0.0 | 5.0 | 5.0 | 5.0 | 0.0 | 5.0 | 5.0 | 5.0 | 5.0 | 0.0 |
| Caudal-fin rays | 14.0 | 14.0 | 14.0 | 0.0 | 12.0 | 14.0 | 13.8 | 0.6 | 13.0 | 13.0 | 14.0 | 13.9 | 0.3 |

*Note:* BI: Biguaçu; DU: d'Una; Hol: holotype; TU: Tubarão.

GGG AAA GCC CCG GCA G-3′) and H7271-COXI (5′-TCC TAT GTA GCC GAA TGG TTC TTT T-3′) (Melo *et al*., 2011). PCR was performed in a solution with a total volume of 25 μl: 2 μl of DNA template, 14.5 μl of PCR Master Mix (Invitrogen, Carlsbad, CA, USA), 1.25 μl of each primer and 6 μl of nuclease-free water to complete the total volume. Some samples were amplified using 1.2 μl of $MgCl^{+2}$ and a lower amount of water (4.8 μl).

The PCR amplifications consisted of a modified protocol from Melo *et al*. (2011), using Invitrogen's Master Mix instructions. Amplification consisted of an initial denaturation step (4 min at 94°C) followed by 40 cycles of chain denaturation (30 s at 95°C), annealing (20 s at 48 and 46°C each) and nucleotide extension (60 s at 72°C). After the cycles, the final extension step was performed at 72°C for 10 min. The PCR products were identified by electrophoresis in a 1% agarose gel, and successful DNA amplifications were sent to Functional Biosciences (Madison, WI, USA) for further purification and sequencing.

Newly generated sequences were edited, and forward and reverse reads were assembled and visualized using Geneious v. 8.1 (http://www.geneious.com; Kearse *et al*., 2012). Under default parameters, all sequences were aligned using the MUSCLE algorithm (Edgar, 2004) also in Geneious. Two alignments were generated, including or excluding outgroup sequences, to assess the influence of these differences in species delimitation results. Therefore, two different data sets (alignments) were analysed, one containing the newly sequenced specimens of *Epactionotus* and additional COI sequences from five individuals of *Epactionotus* available in GenBank provided by Cramer *et al*. (2007, 2011) and the other containing 12 sequences representing 8 species of the related genus *Eurycheilichthys* also from Cramer *et al*. (2007, 2011) (Supporting Information Table S1).

The calculation of genetic distances within and among species was performed using MEGA v. 7.0.26. (Kumar *et al*., 2016) under Kimura 2-parameter + G + I model (Kimura, 1980), which was the best-fit substitution model selected for the data set according to the Bayesian information criterion (BIC).

## 2.5 | Phylogenetic and species delimitation analyses

Alignment of the mitochondrial gene *coI* was partitioned by codon position, and the best model of nucleotide substitution and partition

schemes was evaluated using PartitionFinder v. 2.1.1 (Lanfear *et al*., 2016) under BIC. Phylogenetic relationships between haplotypes were inferred in BEAST v. 2.5 (Bouckaert *et al*., 2019) using a strict molecular clock and Yule process tree prior. Markov chain Monte Carlo analyses ran for 10 million generations, and a single best tree was saved every 10,000 generations. Run stabilization (Effective Sample Size > 200) was checked using Tracer v. 1.7 (Rambaut *et al*., 2018). The first 10% of runs were discarded as burn-in, and the remaining trees were summarized using the maximum clade credibility tree function in TreeAnnotator 2.5 (Bouckaert *et al*., 2019). The gene *coI* was analysed assuming an evolutionary rate of 0.01 per site per Myr (million years) following mutation rates previously proposed to mitochondrial markers in fishes (Bermingham *et al*., 1997). For evaluating genetic data under a mixed method that delimits species based on coalescence and indicates diversification based on a Yule model, the generalized mixed Yule coalescent method (GMYC; Fujisawa & Barraclough, 2013) was applied using the ultrametric tree obtained in BEAST. For GMYC analyses, the package "splits" (Species Limits by Threshold Statistics; Ezard *et al*., 2009) (http://r-forge.r-project.org/projects/splits) was used in programme R version 3.0.0 (R Core Team, 2013). GenBank accession numbers are presented in Supporting Information Table S1.

## 3 | RESULTS

### 3.1 | Morphological analyses

Measurements and counts obtained for species/populations from each of the eight drainages are presented in Tables 1–4. Box plots of the significantly variant meristic data, results of the Tukey's pair-wise tests and median abdominal plate data are shown in Figure 10. When the different means of meristic data were compared between groups, the ANOVA disclosed statistically significant variation in the number of both right and left premaxillary teeth ($f$ = 6.435, $P$ = 3.07E-06 and $f$ = 6.078, $P$ = 6.64E-06, respectively, Figure 10a), number of both right and left dentary teeth ($f$ = 8.331, $P$ = 5.91E-08 and $f$ = 6.28, $P$ = 4.28E-06, respectively, Figure 10b), number of plates in dorsal series ($f$ = 8.02, $P$ = 1.11E-07, Figure 10c), number of plates in median lateral series ($f$ = 5.99, $P$ = 8.03E-06, Figure 10d), number of plates in mid-ventral series ($f$ = 8.276, $P$ = 6.61E-08, Figure 10e), number of plates in ventral series ($f$ = 9.534, $P$ = 5.50E-09, Figure 10f), number of unpaired predorsal plates ($f$ = 12.28, $P$ = 3.47E-11, Figure 10g) and number of both right and left abdominal plates ($f$ = 18.36, $P$ = 3.67E-18 and $f$ = 22.2, $P$ = 2.91E-21, respectively, Figure 10h). With regard to the number of plates in the mid-dorsal series, plates between anal- and caudal-fin series, plates along both dorsal- and anal-fin bases, predorsal plates, number of medium abdominal plates and number of caudal-fin rays, the analysis found no statistically significant variance. Morphometric variables not associated with sexual dimorphism (after Aitchison, 1986, log-ratio transformation) were used in a permutation test (PERMANOVA), PCA and LDA. The results of PERMANOVA with pair-wise $P$-values showed significant values of Euclidean distances ($P$ < 0.05) between almost all groups, except between *Epactionotus* UR and TU ($P$ = 0.0832; Table 5).

When analysing the general patterns of variation among specimens, plots of factor scores of principal components 1 *vs*. 2 grouped specimens into four clusters, partially overlapping each other (Figure 11). The specimens from Biguaçu (*Epactionotus* BI) and d'Una (*Epactionotus* DU) form two overlapping clusters that are well separated from all other populations, having low loadings on PC1. Individuals from Maquiné (part of *E. bilineatus*) and Urussanga (*Epactionotus* UR) form two clusters well separated from each other but with both clouds slightly overlapping with specimens from Tubarão drainage (*Epactionotus* TU). The remaining specimens from Três Forquilhas (other part of *E. bilineatus*), Mampituba (*E. itaimbezinho*), Araranguá (*E. gracilis*) and Tubarão (*Epactionotus* TU) were grouped together. The first two principal components (PC1 and PC2) represent variances of 24.3% and 16.9%, respectively. Measurements with heavier loadings on PC1 were caudal-peduncle width (0.47), body width (0.29), caudal-peduncle length (−0.25) and predorsal length (−0.23). On PC2, heavier loadings were caudal-peduncle width (0.59), pectoral–pelvic fin distance (0.24), suborbital depth (−0.40) and dorsal-fin base length (−0.26).

When evaluating patterns of body shape variation between groups defined by drainage basin populations, the LDA recognized seven distinct clusters, with an overlap between Araranguá (*E. gracilis*) and Mampituba (*E. itaimbezinho*) and with one point of contact shared between part of *E. bilineatus* (from Três Forquilhas) and *E. itaimbezinho* and *Epactionotus* BI and *Epactionotus* DU, respectively (Figure 12). The percentages of separation obtained for each discriminant function (from LD1 to LD4) were 45.8%, 26.1%, 12.6% and 9.5%, respectively. The loadings for discriminant function LD1 indicate caudal-peduncle length (0.01), predorsal length (0.009), first pelvic-fin unbranched ray length (−0.09) and caudal-peduncle width (−0.01) as the more significant measurements. As for LD2, heavier loadings were SL (0.41), internares width (0.39), suborbital depth (−0.01) and dorsal-fin base length (−0.009).

### 3.2 | Phylogenetic and time–divergence analyses

The mitochondrial gene *coI* was sequenced for 23 individuals of *Epactionotus*, each sequence having 731 bp. The best-fit model of nucleotide substitution estimated by PartitionFinder (Supporting Information Table S2) for the first codon is K80 in the data set including *Epactionotus* + *Eurycheilichthys* and JC in the data set including only *Epactionotus*. When partitioned by the second codon, the best-fit model is HKY + I, and when partitioned by the third codon, the best-fit model is HKY + G + I for both data sets. Analyses indicate two species-inclusive clades of *Epactionotus*, one with weak support [posterior probability (PP) = 0.45; Figure 13a; PP = 0.67; Figure 13b, Supporting Information Figures S2 and S3]. One of these clades contains *E. itaimbezinho* and *E. gracilis* (including specimen from Urussanga), both species being reciprocally monophyletic. In the other clade, *E. bilineatus* consists of two reciprocally monophyletic highly supported groups representing populations in the Maquiné and Três Forquilhas River drainages, respectively (PP = 1.0; Figure 13).

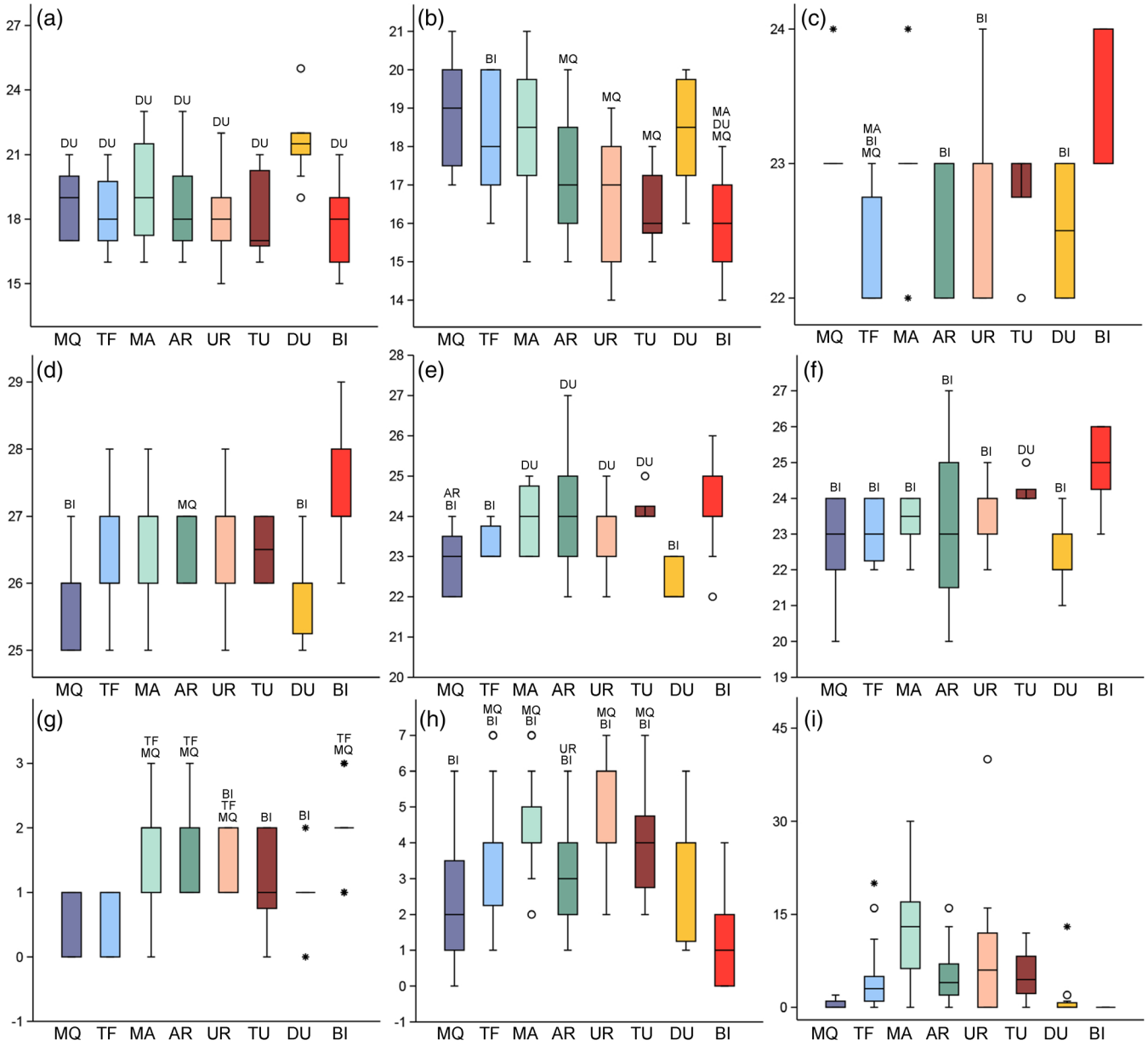


**FIGURE 10** Box plots of the significant variable meristic data between different drainages according to Tukey's pair-wise results. Each graphic contains the number of (a) both right and left premaxillary teeth, (b) both right and left dentary teeth, (c) plates in dorsal series, (d) plates in median lateral series, (e) plates in mid-ventral series, (f) plates in ventral series, (g) unpaired predorsal plates, (h) both right and left abdominal plates and (i) median abdominal plates. Letters above each box indicate species/populations that show statistically significant differences according to the Tukey's pair-wise results. Horizontal line inside each box indicates median values, and short horizontal lines represent minimum and maximum values less than 1.5 times the height of the box; circles represent outliers, and black stars indicate outlier values higher than three times the height of the box

*E. bilineatus* is sister to a group formed by *Epactionotus* BI and the populations of *Epactionotus* TU and *Epactionotus* DU (having *Epactionotus* TU and *Epactionotus* DU as sister lineages in the analyses including only *Epactionotus* sequences; Figure 13; Supporting Information Figures S2 and S3). The most recent common ancestor to *Epactionotus* is dated to the Pleistocene (1.54 Ma, 95% C.I. 1.92–1.15 Ma; Figure 13). Events of divergence between allopatric populations of *E. bilineatus* from Maquiné and Três Forquilhas River drainages are dated to 0.98 Ma (95% C.I. 1.31–0.65 Ma).

### 3.3 | Species delimitation and genetic distance

Results of the GMYC analyses vary depending on the data set used, being more conservative with the matrix containing the outgroup *Eurycheilichthys* (four clusters, *i.e.*, groups including more than two samples, one single entity, *i.e.*, singleton; Table 6; Figure 13b; Supporting Information Figure S3) when compared to the analyses where only *Epactionotus* specimens were examined (five clusters and two single entities; Table 6; Figure 13a; Supporting

**TABLE 5** Results of permutation test (PERMANOVA) with pair-wise *P*-values

| | 1 | 2 | 3 | 4 | 5 | 6 | 7 | 8 |
|---|---|---|---|---|---|---|---|---|
| 1. *Epactionotus bilineatus* (MQ) | | | | | | | | |
| 2. *E. bilineatus* (TF) | 0.0001 | | | | | | | |
| 3. *Epactionotus itaimbezinho* (MA) | 0.0001 | 0.0002 | | | | | | |
| 4. *Epactionotus gracilis* (AR) | 0.0001 | 0.0002 | 0.0024 | | | | | |
| 5. *Epactionotus* (UR) | 0.0001 | 0.0001 | 0.0001 | 0.0001 | | | | |
| 6. *Epactionotus* (TU) | 0.0188 | 0.0007 | 0.0075 | 0.0437 | **0.0832** | | | |
| 7. *Epactionotus* (DU) | 0.0001 | 0.0001 | 0.0001 | 0.0001 | 0.0001 | 0.0002 | | |
| 8. *Epactionotus advenus* (BI) | 0.0001 | 0.0001 | 0.0001 | 0.0001 | 0.0001 | 0.0001 | 0.0001 | |

*Note*: Uncorrected significances of Euclidean distances. Boldface represents value not significant. AR: Araranguá; BI: Biguaçu; DU: d'Una; MA: Mampituba; MQ: Maquiné; TF: Três Forquilhas; TU: Tubarão; UR: Urussanga.

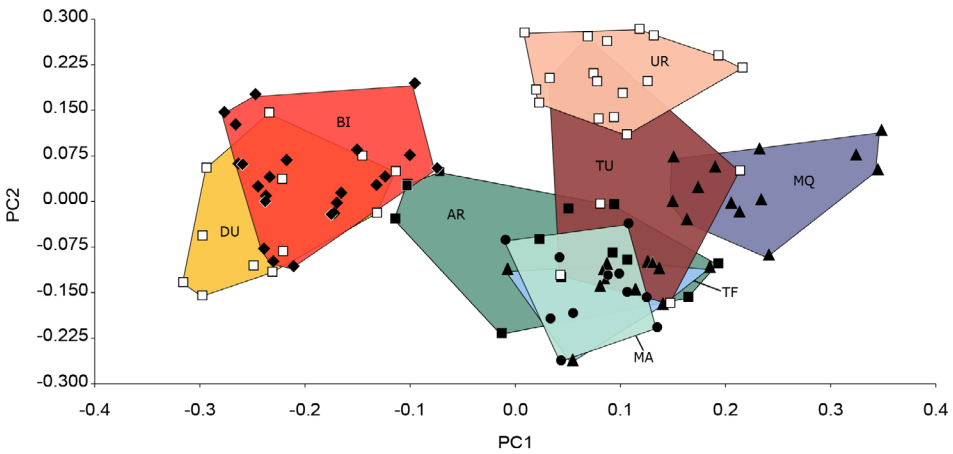


**FIGURE 11** Plots of factor scores of PCA of the species/populations of *Epactionotus*. Triangles, *Epactionotus bilineatus* (MQ and TF); dots, *Epactionotus itaimbezinho* (MA); black squares, *Epactionotus gracilis* (AR); opened squares, populations of *Epactionotus* from Urussanga (UR), Tubarão (TU) and d'Una (DU); diamonds *Epactionotus advenus* (BI)

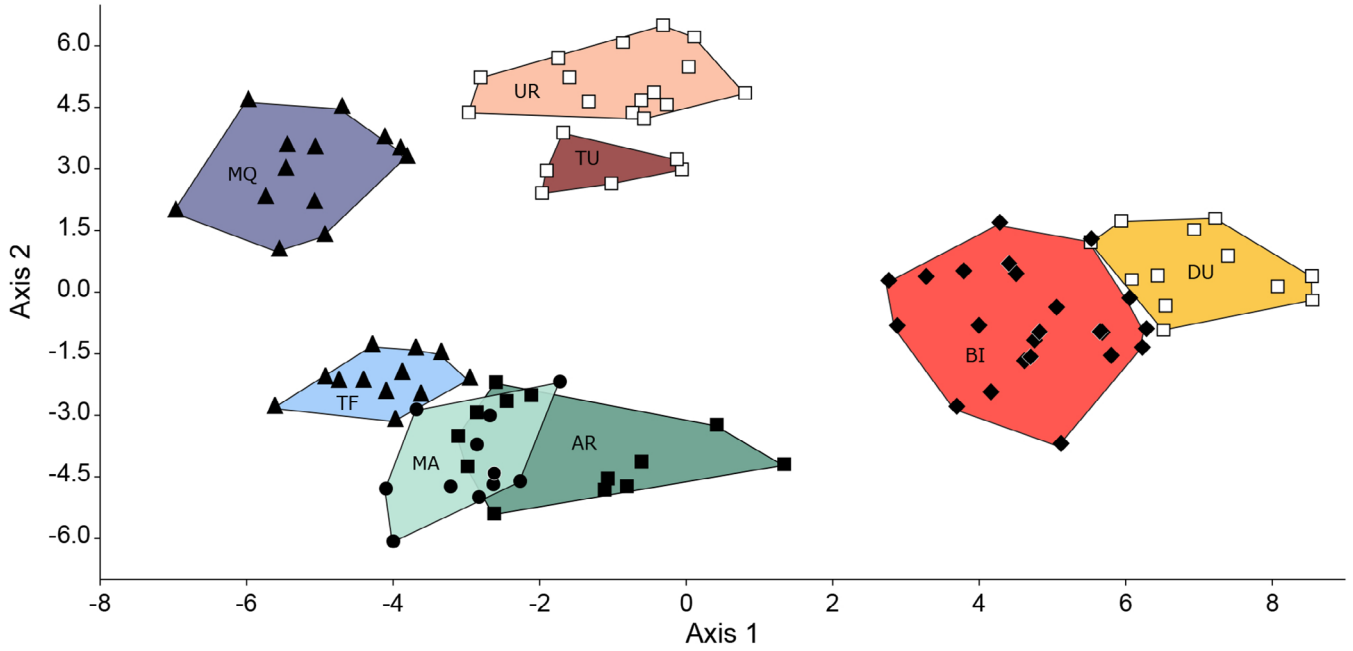


**FIGURE 12** Plots of factor scores of discriminant analysis (linear discriminant analysis) of the species/populations of *Epactionotus*. Triangles, *Epactionotus bilineatus* (MQ and TF); dots, *Epactionotus itaimbezinho* (MA); black squares, *Epactionotus gracilis* (AR); opened squares, populations of *Epactionotus* from Urussanga (UR), Tubarão (TU) and d'Una (DU); diamonds *Epactionotus advenus* from Biguaçu (BI)

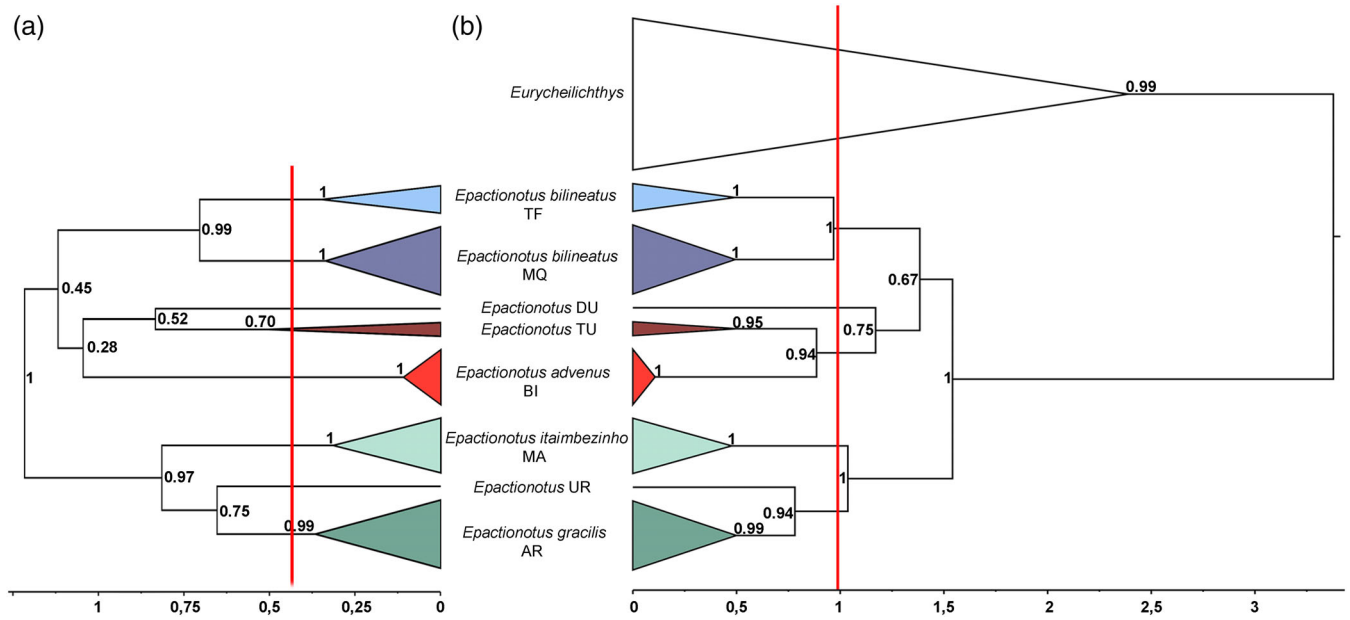


**FIGURE 13** Bayesian phylogenetic tree of species/populations of *Epactionotus* obtained with mitochondrial (cytochrome c oxidase subunit I) locus of (a) all species/populations of *Epactionotus* (likelihood of null model: 67.08211 and maximum likelihood of GMYC model: 69.00491) and (b) all *Epactionotus* plus *Eurycheilichthys* (likelihood of null model: 90.91459 and maximum likelihood of GMYC model: 91.2191). The vertical red line is the single threshold in the general mixed Yule coalescent model (GMYC) test with pure-birth speciation models, where nodes before and after the threshold represent speciation and coalescent events, respectively. Colours correspond to each basin, and node numbers correspond to BI posterior probability (PP). The bar below corresponds to divergence–time estimates in millions of years

**TABLE 6** Comparison of GMYC support for species/populations between different data sets

| Species (drainage) | *Epactionotus* | *Epactionotus* + *Eurycheilichthys* |
|---|---|---|
| *Epactionotus bilineatus* (MQ) | **0.5** | 0.16 |
| *E. bilineatus* (TF) | **0.46** | 0.17 |
| *Epactionotus itaimbezinho* (MA) | **0.53** | **0.27** |
| *Epactionotus gracilis* (AR) | **0.36** | 0.03 |
| *Epactionotus* (UR) | Singleton | Singleton |
| *Epactionotus* (TU) | 0.21 | 0.08 |
| *Epactionotus* (DU) | Singleton | Singleton |
| *Epactionotus advenus* (BI) | **0.62** | 0.89 |

*Note:* Boldface represents groups that were found as clusters using the single threshold in GMYC (generalized mixed Yule coalescent). AR: Araranguá; BI: Biguaçu; DU: d'Una; MA: Mampituba; MQ: Maquiné; TF: Três Forquilhas; TU: Tubarão; UR: Urussanga.

Information Figure S2). Clusters in the analyses containing *Eurycheilichthys* correspond to morphologically delimited species (*e.g.*, *E. bilineatus*, *E. gracilis* and *E. itaimbezinho*) except for the clustering of *Epactionotus* BI with samples of *Epactionotus* TU. The analysis of only *Epactionotus* sequences (excluding *Eurycheilichthys*) supports less-conservative species delimitation and suggests species clusters for most drainages, such as the separation between Maquiné and Três Forquilhas populations in *E. bilineatus* (Table 6; Figure 13a; Supporting Information Figure S2). According to BIC = 3585.7567, the best nucleotide model selected for the genetic distance analysis was K2 + G + I. Distance values within drainages (Table 7) ranged from 0.00% (within individuals of *Epactionotus* BI) to 0.78% (within *E. bilineatus* TF). As for between drainages, distance values varied from 1.2% and 1.5% (between populations of *Epactionotus* TU and *Epactionotus* DU and between *E. bilineatus* from Três Forquilhas and Maquiné, respectively) to 4.07% (between *Epactionotus* BI and *Epactionotus* UR). Genetic distances within species (Table 8) ranged from 0.00% (within individuals of *Epactionotus* BI) to 1.02% (within *E. bilineatus*) and between species ranged from 1.83% (between *E. gracilis* and *E. itaimbezinho*) to 3.33% (between *E. itaimbezinho* and *Epactionotus* BI).

## 3.4 | Taxonomic remarks

The verification and search for diagnostic characters allowed a re-diagnosis of *Epactionotus* based on the absence of expanded fleshy flap on the dorsal surface of the first pelvic-fin ray of males, possession of accessory oral teeth, presence of two longitudinal light stripes on the dorsal surface of the head and trunk, the neural spine of seventh vertebra contacting the unpaired predorsal plate anterior to the nuchal plate, dorsal-fin proximal radial contacting the eighth vertebra and absence of the connecting bone.

**TABLE 7** Pair-wise mtDNA genetic distance values (mean ± s.e.) for cytochrome c oxidase subunit I *coi* gene between and within species/populations according to drainage using a Kimura 2 + G + I parameter

| | Populations | 1 | 2 | 3 | 4 | 5 | 6 | 7 | 8 |
|---|---|---|---|---|---|---|---|---|---|
| 1 | ***Epactionotus bilineatus* (MQ)** | **0.36 ± 0.33** | | | | | | | |
| 2 | *E. bilineatus* (TF) | 1.50 ± 0.48 | 0.78 ± **0.46** | | | | | | |
| 3 | *Epactionotus gracilis* (AR) | 2.51 ± 0.29 | 2.78 ± 0.29 | **0.45 ± 0.32** | | | | | |
| 4 | *Epactionotus* (DU) | 1.90 ± 0.23 | 2.03 ± 0.27 | 1.75 ± 0.34 | - ± - | | | | |
| 5 | *Epactionotus* (TU) | 1.80 ± 0.31 | 2.08 ± 0.40 | 1.72 ± 0.39 | 1.20 ± 0.01 | **0.73 ± 0.00** | | | |
| 6 | *Epactionotus* (UR) | 3.19 ± 0.15 | 3.58 ± 0.10 | 1.57 ± 0.20 | 2.05 ± 0.00 | 2.04 ± 0.20 | - ± - | | |
| 7 | *Epactionotus itaimbezinho* (MA) | 2.52 ± 0.40 | 2.80 ± 0.49 | 1.83 ± 0.28 | 2.15 ± 0.27 | 1.83 ± 0.26 | 2.09 ± 0.14 | **0.42 ± 0.31** | |
| 8 | *Epactionotus advenus* (BI) | 2.51 ± 0.38 | 2.94 ± 0.56 | 3.30 ± 0.32 | 2.62 ± 0.00 | 2.20 ± 0.22 | 4.07 ± 0.00 | 3.33 ± 0.38 | 0.00 ± **0.00** |

*Note*. Diagonal boldface numbers show within-drainage values. Blue and red numbers show lowest and highest genetic distance values, respectively, between and within drainages. AR: Araranguá; BI: Biguaçu; DU: d'Una; MA: Mampituba; MQ: Maquiné; TF: Três Forquilhas; TU: Tubarão; UR: Urussanga.

**TABLE 8** Pair-wise mtDNA genetic distance values (mean ± s.e.) for cytochrome c oxidase subunitI gene between and within species using a Kimura 2 + G + I parameter

| | Species | 1 | 2 | 3 | 4 |
|---|---|---|---|---|---|
| 1 | ***Epactionotus bilineatus* (MQ + TF)** | 1.02 ± **0.69** | | | |
| 2 | *Epactionotus gracilis* (AR) | 2.61 ± 0.32 | **0.45 ± 0.32** | | |
| 3 | *Epactionotus itaimbezinho* (MA) | 2.62 ± 0.45 | 1.83 ± 0.28 | **0.42 ± 0.31** | |
| 4 | *Epactionotus advenus* (BI) | 2.67 ± 0.50 | 3.30 ± 0.32 | 3.33 ± 0.38 | 0.00 ± **0.00** |

*Note:* Diagonal boldface numbers show within-drainage values. Blue and red numbers show the lowest and highest genetic distance values, respectively, between and within drainages. AR: Araranguá; BI: Biguaçu; MA: Mampituba; TF: Três Forquilhas; MQ: Maquiné.

After iterative analyses were performed, the three formerly described species *E. bilineatus*, *E. gracilis* and *E. itaimbezinho* were recognized. Even though different lines of evidence that suggest separation between the allopatric populations of *E. bilineatus* (Maquiné and Três Forquilhas) were observed, the GMYC approach (using the tree with *Eurycheilichthys*), its reciprocal monophyly and external morphology (*e.g.*, wider head and body and broader longitudinal light stripe markings on the head and predorsal region when compared to others), suggests both populations (Maquiné and Três Forquilhas) are a single species. Regarding the newly discovered populations, individuals sampled from the Urussanga River were variably delimited and varied in their relationships to other species/populations, because morphological analyses (PCA and LDA) indicate that they are more similar to *Epactionotus* TU, and the GMYC analysis shows a closer relationship to *Epactionotus gracilis*. In addition, in spite of having larger samples for morphological analyses (>10 individuals), the same was not found for the population from Tubarão. Therefore, any taxonomic circumscription for these groups is avoided at this time. Future studies should aim to expand sampling of these populations and consider both morphological and molecular data. Due to the support from both molecular analyses (*e.g.*, GMYC analysis and sequence divergence estimates) and morphological data (*e.g.*, measurements and meristics) including discrete features (see the "Diagnosis" section), this study proposes the population from the Biguaçu River as a new species, formally described here.

## 3.5 | Species description

*Epactionotus advenus*, new species.

urn:lsid:zoobank.org:act:1AA51A28-3B9F-4F1A-B502-F3C2BDCFCE42

See Figure 9 and Tables 2 and 4.

### 3.5.1 | Holotype

UFRGS 28220, female, 35.4 mm SL, Brazil, Santa Catarina, Antônio Carlos, Rachadel River and a small tributary, Biguaçu drainage, inside property of Mr. Paulo Lopes at locality of Guiomar, 27° 29′ 44″ S, 48° 46′ 57″ W, 2 August 2015, T. P. Carvalho, F. Carvalho and A. Thomaz.

### 3.5.2 | Paratypes

UFRGS 20926 (11, 32.7–39.0 mm SL + 3 fixed in alcohol) and MCP 54449 (4, 36–37.9 mm SL + 2 c&s, 35.4–36.1 mm SL), collected with holotype. UFRGS 22913 (9, 30.8–37.8 mm SL + 8 fixed in alcohol), Brazil, Santa Catarina, Antonio Carlos, Rachadel River, north of Rachadel, 27° 28′ 22.8″ S, 48° 48′ 00.8″ W, 30 May 2017, J. Ferrer, L. Donin, N. Pio and T. P. Carvalho.

### 3.5.3 | Diagnosis

*E. advenus* is distinguished from *E. bilineatus*, *E. itaimbezinho* and *E. gracilis* by having the posterior region of the abdomen naked, devoid of any embedded platelets between the pelvic fins and anal tube (*vs*. at least one small platelet between the pelvic fins and anal tube). In addition, it can be distinguished from *E. bilineatus* and *E. itaimbezinho* by having comparatively narrower light stripes on the head, predorsal region and dorsal surface of the trunk (*vs*. broader light stripe markings); a narrower body (cleithral width 19%–20.8% *vs*. 23.1%–26.1% and 22.2%–23.8% SL, respectively); and a shorter pectoral-fin spine (15.5%–18.8% *vs*. 20.2%–23.1% and 19.1%–21.6% SL, respectively). It can be distinguished from *E. itaimbezinho* and *E. gracilis* by a shallower caudal peduncle (7.7%–9.3% *vs*. 9.9%–11.2% and 9.8%–10.9% SL, respectively); by having the chromatophores of the first thickened rays of the dorsal, pectoral and pelvic fins evenly arranged and distributed, leaving fin rays plain and dusky (*vs*. chromatophores arranged in a series of five to six small dots); and by the completely dark-brown ventral lobe of the caudal fin (*vs*. ventral lobe of caudal fin dark-brown with hyaline spots in the middle portion of the interradial membrane between the two most ventral rays – Figure 14). It is also differentiated from *E. bilineatus* by a narrower head (59.5%–66.6% *vs*. 70.2%–77.2% HL). The new species can be distinguished from the populations of *Epactionotus* UR and *Epactionotus* TU by the posterior region of the abdomen naked, devoid of any embedded platelets between the pelvic fins and anal tube (*vs*. at least one small platelet between the pelvic fins and anal tube). The species can be distinguished from the populations of *Epactionotus* UR and of *Epactionotus* DU by the ventral lobe of caudal-fin completely dark brown (*vs*. ventral lobe of the caudal fin dark-brown with hyaline spots in the middle portion of the interradial membrane between the two most ventral rays – Figure 14). In addition, it is distinguished from the population of *Epactionotus* TU by having a shorter pectoral-fin spine (15.5%–18.8% *vs*. 19.3%–20.7% SL), narrower head (59.5%–66.6% *vs*. 67.1%–71.6% SL), smaller interorbital distance (34.5%–38.6% *vs*. 39.1%–41.2% HL) and narrower body (cleithral width 19.0%–20.8% *vs*. 22.1%–24.3% SL).

Other slightly overlapping features useful to distinguish the new species are as follows: *E. advenus* is distinguished from *E. bilineatus* by a shallower caudal peduncle (7.7%–9.3% *vs*. 9.2%–10.8%), smaller interorbital distance (34.5%–38.6% *vs*. 38.4%–42.3% HL), shorter pectoral-fin length (19.0%–22.3% *vs*. 22.3%–26.1% SL) and shorter first pelvic-fin unbranched ray length (13.6%–16.5% *vs*. 16.3%–19.4% SL). Finally, it can be distinguished from the *Epactionotus* UR population by a narrower body (cleithral width 19.0%–20.8% *vs*. 20.6%–22.8%), and it is also distinguished from the *Epactionotus* TU population by a shorter pectoral-fin length (19.0%–22.3% *vs*. 22.3%–23.5% SL) and shallower caudal peduncle (7.7%–9.3% *vs*. 9.3%–10.7% SL).

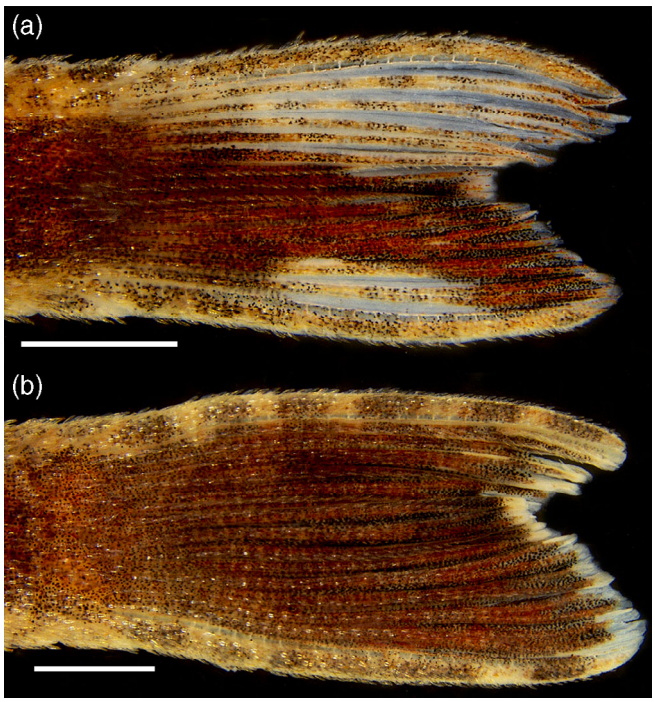


**FIGURE 14** Caudal-fin colour variation in species/populations of (a) *Epactionotus gracilis* (AR), UFRGS 22945, 28.2 mm standard length (SL); (b) *Epactionotus advenus* (BI), MCP 54449, 37.8 mm SL. Scale = 2 mm

### 3.5.4 | Description

Measurements and counts are presented in Tables 2 and 4. Body relatively slender and elongate. Dorsal profile of head and body slightly convex from snout tip to dorsal-fin origin; interorbital slightly elevated. Trunk profile mostly straight and slightly tapering from dorsal-fin origin to anteriormost procurrent caudal-fin ray. Body deepest at dorsal-fin origin and shallowest at posterior portion of caudal peduncle. Caudal peduncle ovoid to rounded in cross-section, progressively compressed from anteriormost anal-fin ray to caudal-fin base. Greatest body width at cleithrum.

Anterior margin of snout rounded and head narrow in dorsal view. Snout with paired depressions anterior to nostrils; depression beginning close to snout tip. Eye small, dorsolaterally positioned, iris operculum present. Fenestrae of compound pterotic increasing in size towards posterolateral margin of bone. Four to five (usually four) paired predorsal plates and one to three (usually two) unpaired predorsal plates anterior to square-shaped nuchal plate. Odontodes on margin of snout slightly larger than remaining odontodes on head.

Odontodes on ventral margin of snout distinctly enlarged. Posterior tip of parieto-supraoccipital without small tuft of enlarged odontodes. No other crests of odontodes on dorsal surface of head. Lips rounded and covered with globular papillae; small fleshy ridge posterior to dentary. Maxillary barbel short. Teeth slender, bifid, with blade-like larger medial cusp and smaller lateral cusp.

Accessory patch of unicuspid teeth on both premaxilla and dentary, located more internally in mouth and attached to dermal bone. Accessory teeth elongate, sharply pointed, directed posteroventrally (on premaxilla) and anteroventrally (on dentary).

Median series of lateral plates complete; some median lateral plates without lateral line canal; lateral line gap starting at vertical line through midpoint of dorsal fin. Odontodes on head and trunk pointed, uniform in size and shape and somewhat aligned; odontodes on trunk and caudal peduncle slightly larger. Odontodes on ventral surface of body smaller and evenly distributed, not arranged in lines. Body almost entirely covered by plates, except nostrils, area between lower lip and pectoral girdle, region overlying lateral opening of swimbladder capsule, most of abdomen, area around anus, and fin bases. Ventral portions of cleithrum and coracoid almost entirely exposed and supporting odontodes, except for small median region, especially of cleithrum, covered with skin. Abdomen with none to four (usually one) small, rounded to slightly laterally elongate lateral abdominal plates, located between posterior process of coracoids and pelvic-fin insertions; median and posterior region of abdomen between pelvic fins and urogenital papilla naked, devoid of any plates or platelets embedded in skin or scattered odontodes. Total vertebrae 31, ribs 5, beginning on eighth or ninth vertebral centrum, in addition to large rib on sixth centrum.

Dorsal fin I,7 (one specimen with I,8), its origin at vertical through middle of pelvic fin. Dorsal-fin spinelet short and slightly wider than dorsal-fin spine. Pectoral fin I,6, with large axillary slit in skin behind fin insertion. Serrae absent along mesial margin of pectoral-fin spine. Pectoral fin reaching to vertical line slightly posterior to insertion of pelvic-fin unbranched ray in males; reaching to midpoint of pelvic-fin unbranched ray in females. Pelvic fin i,5, with robust first ray shorter than branched rays. Skin flap absent on first unbranched pelvic-fin ray of males and females. First pelvic-fin unbranched ray slightly thicker in males than females (see the "Sexual dimorphism" section). Anal fin i,5; first anal-fin pterygiophore usually exposed in front of unbranched fin ray. Odontodes on pelvic-fin unbranched ray turned and strongly pointing mesially. Adipose fin absent. Caudal fin i,14,i (one specimen with i,13,i), forked, lower lobe equal to or slightly longer than upper lobe.

### 3.5.5 | Colouration in alcohol

Ground colour of dorsal surface of head and trunk medium to dark greyish brown, yellowish white and mostly unpigmented ventrally. Pair of longitudinal light-cream stripes on each side of snout; stripes begin medially on tip of snout, passing laterally between nostrils and orbits on each side, and proceed backward, narrowing after orbit and terminating near posterior margin of compound pterotic. Second pair of longitudinal light stripes on each side of dorsal surface of body from predorsal region to near caudal peduncle. Lateral margins of head and trunk, especially head, below line from ventral margin of snout to posterior tip of opercular bone and tip of posterior process of cleithrum lighter than dorsal portions of head, but with scattered small dark dots. Posterior tip of parieto-supraoccipital slightly unpigmented. First thickened rays of dorsal, pectoral and pelvic fins with chromatophores equally arranged and

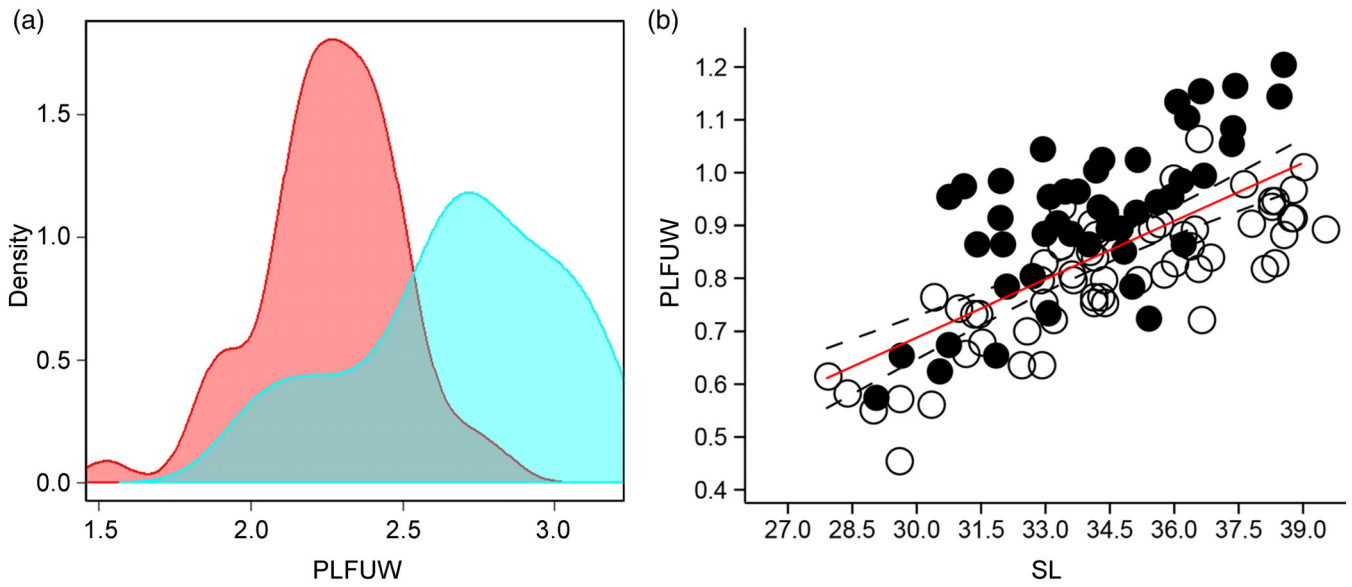


**FIGURE 15** Sexual dimorphism in *Epactionotus* species/populations identified by VARSEDIG algorithm. (a) Distribution of the first pelvic-fin unbranched ray width (PLFUW) for males (blue) and females (red) and (b) bivariate plot of PLFUW against standard length (SL) for males (dots) and females (circles)

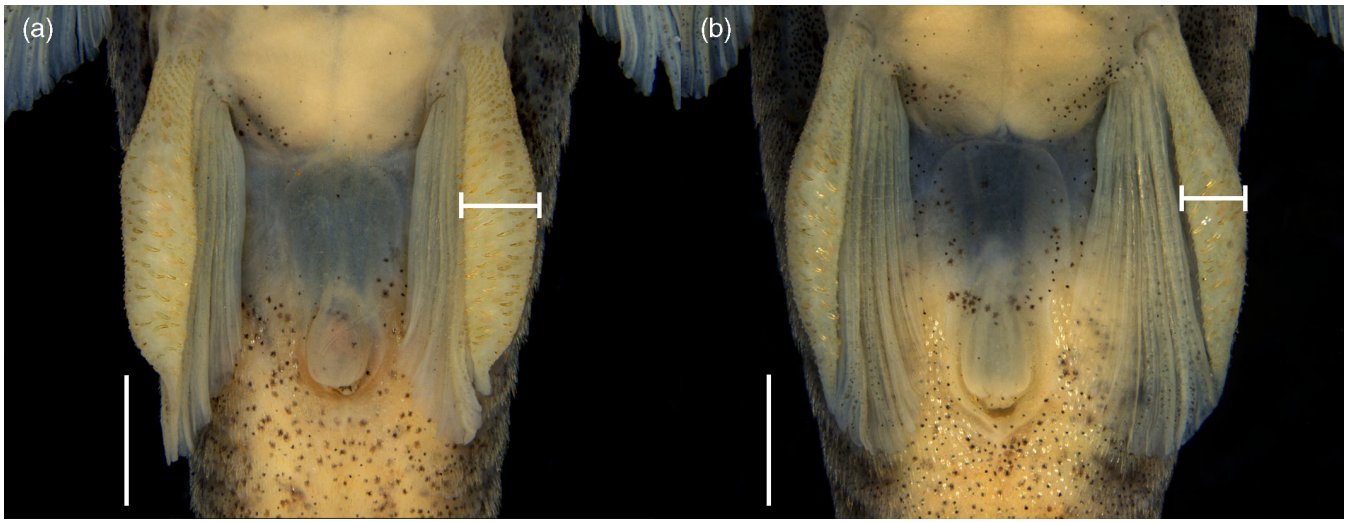


**FIGURE 16** Pelvic region of *Epactionotus advenus* from Biguaçu. First pelvic-fin unbranched ray slightly thicker in males than females. (a) Male, MCP 54449, 36 mm standard length (SL); (b) female, UFRGS 20926, 39 mm SL. Ventral view, anterior towards top. Scale = 2 mm

**FIGURE 17** Collection locality and habitat of *Epactionotus advenus* from Biguaçu, Rachadel River at Antonio Carlos, north of Rachadel, Santa Catarina State, Brazil (27° 28′ 22.8″ S, 48° 48′ 00.8″ W)

distributed, leaving fin rays plain and dusky. Branched rays in these fins with similar colour pattern. Dorsal and ventral borders of pectoral-fin slit densely pigmented with brownish black chromatophores forming dark blotches of irregular shape and size. Concentration of black chromatophores on ventral side of pectoral girdle, between posterior process of coracoid and origin of pectoral-fin spine. Few dots on leading anal-fin branched ray. Interradial membrane of all fins, except caudal-fin, unpigmented. Ventral lobe of caudal-fin completely dark brown; interradial membrane between five upper rays of caudal fin unpigmented, leaving dorsal lobe lighter towards posterior end.

### 3.5.6 | Sexual dimorphism

Males have a small, conical urogenital papilla behind the anal tube, which is not present in females. Females have a longer pectoral fin than males (pectoral fin of females reaches to the midpoint of pelvic-fin unbranched ray *vs.* pectoral fin of males reaching to a vertical line slightly posterior to the insertion of pelvic-fin unbranched ray). Finally, as identified by the VARSEDIG algorithm, males of *Epactionotus*, including *E. advenus*, have the first pelvic-fin unbranched ray slightly thicker than females' (width of the first pelvic-fin unbranched ray of males 17.7%–21.0%, mean 19.8%, *vs.* 13.4%–17.6%, mean 15.4% of its length in females – Figures 15 and 16).

### 3.5.7 | Distribution

*E. advenus* is so far known from two localities in the Rachadel River, a tributary of the Biguaçu River, in Santa Catarina State, southern Brazil (Figures 1 and 17; Supporting Information Figure S1).

### 3.5.8 | Habitat and ecological notes

*E. advenus* inhabits medium- to fast-flowing clear water of a small creek about 5 m wide with a maximum depth of 0.5 m, running over sand, pebbles and rocks (Figure 17). The specimens were caught in the submersed marginal vegetation consisting of mostly grasses.

*Conservation status*

*E. advenus* is known only from two localities along the same stretch of the Rachadel River. This river basin and its alluvial plain have suffered from deforestation, sand extraction and transformation of its margins into agricultural land. As its distribution is largely unknown and other conservation parameters cannot be accessed for the species, *E. advenus* is provisionally categorized as "data deficient" according to the IUCN criteria and categories (IUCN Standards and Petitions Committee, 2019).

*Etymology*

The specific name *advenus* is from the Latin word *advena*, meaning "stranger," "outsider" and "foreigner," in reference to the non-contiguous distribution of the species with the southward species/populations, an adjective.

## 4 | DISCUSSION

The range extension of *Epactionotus* is expanded considerably northwards from its former northern limit in the Araranguá River basin (Reis & Schaefer, 1998), and the genus is currently known from the Urussanga, Tubarão, d'Una and Biguaçu River drainages. Previous authors (Abell *et al*., 2008; Reis & Schaefer, 1998) have recognized patterns of endemism in the southern Brazilian coastal drainages. The causes of this endemism and the isolation of this fauna are often related to palaeodrainage connections during marine regressions during Pleistocene glacial periods (Thomaz *et al*., 2015; Thomaz & Knowles, 2018; Wendt *et al*., 2019) or the presence of conspicuous mountainous barriers such as the Serra do Tabuleiro (Carvalho, 2007; Thomaz & Knowles, 2020). Despite being likely for other groups of fishes, the distribution of *Epactionotus* cannot be explained solely by these mechanisms, considering its presence on the northward Biguaçu River drainage and the unique genetic groups of each drainage. Other than the palaeodrainage connection by sea-level retreat, an often-cited model of fish dispersal within coastal basins is headwater river capture (Lima *et al*., 2017; Ribeiro, 2006). Nonetheless, headwaters of the Biguaçu are not contiguous with those of the southward tributaries (*e.g*., Tubarão River drainage; Figure 1; Supporting Information Figure S1), and stepping-stone dispersal *via* headwater river captures would require the presence of the genus in intervening drainages, such as the Cubatão Sul River drainage. Two explanations can illustrate this pattern: extinction affected the drainages between Tubarão/d'Una and Biguaçu, or these fishes have not yet been sampled in this area.

The extent of geographic distribution in freshwater fish species seems to be directly related to the position on the river network a fish occupies (Carvajal-Quintero *et al*., 2019). Species such as *Epactionotus* that are ecologically associated with rapids on upstream portions of the river network may be susceptible to isolation and allopatric diversification and, as a result, have smaller distribution ranges. A related factor to divergence is the use, or lack thereof, of river connections on the palaeodrainages during Pleistocene sea-level retreats (Thomaz & Knowles, 2020). *Epactionotus* lineages may not have used this lowland connection due to habitat specificities that created an ecological barrier of lowland habitat between these former palaeodrainages. This is also observed in the genetic signatures of other rapids-dwelling headwater fishes in the region (Hirschmann *et al*., 2015). Therefore, analyses that suggest faster rates of diversification on headwater habitats (Roxo *et al*., 2017) may reflect an association between population genetic differentiation and speciation rates (Harvey *et al*., 2017; Singhal *et al*., 2018).

Analyses of morphological data (ANOVA, PERMANOVA, PCA and LDA) of previously known and new populations support the uniqueness of each of the *Epactionotus* populations/species on isolated river drainages. Similarly, most genetic distance values between drainages are above 2%, and results of the GMYC analyses (*Epactionotus* only) suggest sample clustering for most drainages. Isolated river drainages have been extensively used as biogeographical units (Albert & Carvalho, 2011; Dagosta & Pinna, 2017) and are often a primary hypothesis for species delimitation in freshwater fishes.

On the contrary, when *Eurycheilichthys* is maintained, the GMYC species delimitation varies notably, indicating that the mixed method is weakly conclusive with the data available and also variable according to the number of species tested (da Cruz & Weksler, 2018; Talavera *et al*., 2013). A more comprehensive analysis, in terms of molecular markers and site sampling (*e.g*., d'Una and Tubarão River drainages; Figure 1), will better address the taxonomic issues of the remaining populations of *Epactionotus*.

Indeed, genetic divergence is frequently observed between populations of Neotropical freshwater fishes in isolated drainages (Hirschmann *et al*., 2015; Lima *et al*., 2017; Thomaz *et al*., 2015). Nonetheless, this divergence is not often accompanied or supported by morphological differences (Benine *et al*., 2009; Cherobim *et al*., 2016; Lima *et al*., 2017; Melo *et al*., 2011), especially in this relatively small geographic scale (Hirschmann *et al*., 2015), which contrasts with the analyses in *Epactionotus* that show some morphometric variation among groups (Figures 11 and 12). The morphological features that most strongly distinguish the drainage populations observed here (*e.g*., body shape and dermal plates) can also be associated with adaptations to habitat types and locomotion (Carvalho & Reis, 2011; Fagundes *et al*., 2020; Roxo *et al*., 2017). At a

finer scale, *Epactionotus* shows a range of habitat preferences (*e.g.*, rocky bottoms, marginal vegetation; Reis & Schaefer, 1998; Malabarba *et al.*, 2013), and the association between morphology and ecological features of these drainages can be further explored in future analyses.

When analysing the species and populations of *Epactionotus*, all the diagnostic characters described by Reis and Schaefer (1998) added to the absence of the connecting bone, which is considered another independently derived diagnostic feature of *Epactionotus* (Calegari *et al.*, 2011; Delapieve *et al.*, 2017; Martins *et al.*, 2014; Rodriguez *et al.*, 2015), were observed here. Therefore, in spite of new information provided over the past 20 years, the combination of the diagnostic characters formerly given by Reis and Schaefer (1998) has proven to be useful.

## 4.1Comparative material examined (all from Brazil)

*E. bilineatus*: MCN 12064, 3 alc, rio Pinheiros, Maquiné, Rio Grande do Sul (29° 38′ 17″ S, 50° 13′ 30″ W). MCN 12080, 3 alc, rio Maquiné, Maquiné, Rio Grande do Sul (29° 39′ 07″ S, 50° 12′ 32″ W). MCP 18495, 52 alc, arroio Água Parada, tributary of the rio Maquiné, Maquiné, Rio Grande do Sul (*c.* 29° 40′ S, 50° 12′ W). MCP 19105, 7 alc, arroio do Ouro, on BR-101 *c.* 1 km west from Maquiné (29° 39′ 58″ S, 50° 10′ 59″ W). MCP 21335, 15 alc, arroio Escangalhado, Maquiné, Rio Grande do Sul (29° 34′ 05″ S, 50° 17′ 15″ W). MCP 26964, 2 alc, 2 tis, arroio Água Parada, Maquiné, Rio Grande do Sul (29° 39′ 43″ S, 50° 12′ 43″W). MCP 29116, 25 alc, 3 c&s, arroio Forqueta near mouth of a small tributary of the rio Maquiné, Barra do Ouro, Rio Grande do Sul (29° 32′ 08″ S, 50° 12′ 21″ W). MCP 29119, 9 alc, 3 c&s, arroio Garapiá, *c.* 300 m downstream from waterfall, tributary of rio Forqueta, Maquiné, Barra do Ouro, Rio Grande do Sul (29° 30′ 26″ S, 50° 14′ 39″ W). UFRGS 3290, 1 alc, rio Maquiné, Maquiné, Rio Grande do Sul (29° 40′ 16″ S, 50° 11′ 44″ W). UFRGS 10649, 5 alc, rio Cerrito at Barra do Ouro, Barra do Ouro, Rio Grande do Sul (29° 34′ 14″ S, 50° 16′ 50″ W). UFRGS 17817, 39 alc, Barra do Ouro on the road to Garapiá, Maquiné, Rio Grande do Sul (29° 34′ 13.6″ S, 50° 16′ 49.0″ W). UFRGS 17967, 5 alc, rio Maquiné near camping ground of Maquiné, Maquiné, Rio Grande do Sul (29° 38′ 53″ S, 50° 13′ 04″ W). UFRGS 20804, 6 alc, rio Escangalhado near Barra do Ouro, Barra do Ouro, Rio Grande do Sul (29° 34′ 02″ S, 50° 17′ 09″ W). UFRGS 20943, 18 alc, rio Maquiné at bathing spot, Maquiné, Rio Grande do Sul (29° 39′ 08″ S, 50° 12′ 34″ W). UFRGS 22210, 2 alc, arroio Água Parada at Barra do Ouro, Barra do Ouro, Rio Grande do Sul (29° 40′ 19″ S, 50° 12′ 12″ W). UNICTIO 1406, 8 alc, 1 tis, rio Maquiné, Maquiné, Rio Grande do Sul (29° 35′ 14.7″ S, 50° 16′ 12.0″ W). UNICTIO 1444, 1 alc, 1 tis, arroio Forqueta, Maquiné, Rio Grande do Sul (29° 32′ 28.1″ S, 50° 12′ 08.9″ W). MCN 18573, 39 alc, rio Carvalho inside property of Dona Maria Luiza, São Francisco de Paula, Rio Grande do Sul (29° 22′ 55″ S, 50° 11′ 52″ W). MCN 18598, 8 alc, arroio Bananeira, at bridge on road Rota do Sol, São Francisco de Paula, Rio Grande do Sul (29° 25′ 17″ S, 50° 09′ 56″ W). MCN 18608, 19 alc, arroio Pinto at vicinal road to Rota do Sol, São Francisco de Paula (29° 23′ 22″ S, 50° 10′ 52″ W). MCN 19405, 8 alc, rio Três Forquilhas, Terra de Areia, Rio Grande do Sul (29° 32′ 29″ S, 50° 01′ 54″ W). MCN 19406, 8 alc, rio Três Forquilhas, Terra de Areia, Rio Grande do Sul (29° 32′ 29″ S, 50° 01′ 54″ W). MCN 20068, 5 alc, arroio near to Linha Bernardes, Tramandaí (29° 30′ 50.4″ S, 50° 07′ 42.8″ W). MCP 14806, paratypes, 4 alc, 1 c&s, rio Três Pinheiros, tributary of rio Três Forquilhas, 8 km north-west of highway BR-101 towards Itati, Terra de Areia, Rio Grande do Sul (*c.* 29° 32′ S, 50° 06′ W). MCP 23679, 40 alc, 1 tis, arroio do Padre ca 0.4 km upstream from church Arroio do Padre, Itati, Rio Grande do Sul (29° 29′ 28″ S, 50° 08′ 35″ W). MCP 25277, 5 alc, rio Três Pinheiros, at bridge on road to Vila Itati, *c.* 7 km north of highway BR-101, Terra de Areia, Rio Grande do Sul (29° 31′ 36″ S, 50° 06′ 21″ W). MCP 25311, 34 alc, stream on road between Terra de Areia and Vila Itati, *c.* 8 km north of highway BR-101, Vila Nova, Terra de Areia, Rio Grande do Sul (29° 31′ 01″ S, 50° 06′ 40″ W). MCP 28978, 39 alc, arroio Japonês, between Três Forquilhas and Itati, Três Forquilhas, Rio Grande do Sul (*c.* 29° 32′ S, 50° 05′ W). MCP 29138, 14 alc, arroio Bananeira, tributary of rio Três Forquilhas, Itati, Rio Grande do Sul (29° 27′ 22″ S, 50° 11′ 13″ W). MCP 29293, 29 alc, 3 c&s, arroio Bananeira, tributary of rio Três Forquilhas, Itati, Rio Grande do Sul (29° 25′ 26″ S, 50° 10′ 16″ W). UFRGS 3257, 6 alc, rio Três Forquilhas near Três Forquilhas, Três Forquilhas, Rio Grande do Sul (29° 31′ 60″ S, 50° 04′ 60″ W). UFRGS 6564, 22 alc, rio Três Forquilhas at Vila Boa União, Terra de Areia, Rio Grande do Sul (29° 28′ 17″ S, 50° 07′ 01″ W). UFRGS 9128, 2 alc, rio Carvalho near road Rota do Sol, São Francisco de Paula, Rio Grande do Sul (29° 22′ 55″ S, 50° 11′ 52″ W). UFRGS 12740, 6 alc, rio Três Forquilhas, Três Forquilhas, Rio Grande do Sul (29° 28′ 20.2″ S, 50° 07′ 10.0″ W). UFRGS 16506, 23 alc, mouth of arroio da Barra into arroio Bananeiras, Itati, Rio Grande do Sul (29° 25′ 37″ S, 50° 10′ 49″ W). UFRGS 16538, 14 alc, arroio Carvalho tributary to rio Três Forquilhas on road Rota do Sol, Itati, Rio Grande do Sul (29° 23′ 25″ S, 50° 11′ 02″ W). UFRGS 16545, 2 alc, rio da Boa União, tributary to rio Três Forquilhas at vicinal road to Rota do Sol, upstream Itati, Rio Grande do Sul (29° 27′ 18″ S, 50° 07′ 22″ W). UFRGS 20747, 2 alc, arroio Bananeiras at vicinal road to Rota do Sol, Itati, Rio Grande do Sul (29° 25′ 36″ S, 50° 10′ 29″ W). UFRGS 20827, 11 alc, creek tributary to rio Três Forquilhas on parallel road to Rota do Sul, Itati, Rio Grande do Sul (29° 25′ 54.86″ S, 50° 06′ 42.78″ W). UFRGS 21392, 5 alc, rio do Padre, tributary to rio Três Forquilhas, Itati, Rio Grande do Sul (29° 29′ 27.41″ S, 50° 08′ 49.00″ W). *E. itaimbezinho*: MCP 14708, paratypes, 12 alc, 3 c&s, rio Canoas, tributary of rio Mampituba, *c.* 8 km from Praia Grande towards Mãe dos Homens, Praia Grande, Santa Catarina (*c.* 29° 14′ S, 50° 01′ W). MCP 23620, 19 alc, arroio Maia Coco in Vila Rosa *c.* 5 km north-west of Praia Grande, Morrinhos do Sul, Santa Catarina (29° 10′ 13″ S, 49° 58′ 49″ W). MCP 23683, 36 alc, rio Mangue between Morrinhos do Sul and Praia Grande, Morrinhos do Sul, Santa Catarina (29° 14′ 55″ S, 49° 55′ 30″ W). MCP 29251, 15 alc, stream tributary to rio Mampituba towards Itaimbezinho Canion, Praia Grande, Santa Catarina (29° 12′ 18″ S, 49° 58′ 19″ W). UFRGS 10833, 3 alc, stream tributary to rio Mampituba, Praia Grande, Santa Catarina (29° 10′ 36″ S, 49° 58′ 14″ W). UFRGS 10849, 9 alc, arroio Molha Coco, tributary to rio Mampituba 0.6 km from Praia

Grande at Vila Rosa, Praia Grande, Santa Catarina (29° 10′ 09″ S, 49° 58′ 56″ W). UFRGS 12719, 3 alc, creek on road to Faxinalzinho Canion, Praia Grande, Rio Grande do Sul (29° 11′ 54″ S, 49° 57′ 57″ W). UFRGS 23963, 1 alc, pool near rio Mampituba, Praia Grande, Santa Catarina (29° 15′ 10″ S, 50° 07′ 00″ W). UNICTIO 1908, 1 of 5 alc, 3 tis, arroio Faxinalzinho, tributary to rio Mampituba, Praia Grande, Santa Catarina (29° 14′ 57″ S, 50° 07′ 17″ W). UNICTIO 1993, 1 of 2 alc, 1 tis, arroio Malacara, tributary to rio Mampituba, Praia Grande, Santa Catarina (29° 10′ 07.2″ S, 49° 58′ 17.7″ W). UNICTIO 2123, 1 of 11 alc, 1 tis, arroio Cachoeira, tributary to rio Mampituba, Praia Grande, Santa Catarina (29° 08′ 11.6″ S, 49° 54′ 21.1″ W). *E. gracilis*: MCP 20282, holotype, rio Jordão at Jordão Alto, Nova Veneza, Santa Catarina (*c.* 28° 36′ S, 49° 29′ W). MCP 11615, paratypes, 15 alc, 4 c&s, collected with holotype. MCP 19193, 2 alc, rio do Cedro on road from Meleiro to Forquilhinha, Meleiro, Santa Catarina (*c.* 28° 48′ S, 49° 34′ W). MCP 19198, 1 alc, rio Mãe Luzia, Forquilha, creek tributary of rio Araranguá, Treviso, Santa Catarina (28° 27′ 40″ S, 49° 30′ 04″ W). MCP 23606, 5 alc, rio Morto *c.* 7 km north of Meleiro towards São Francisco, Meleiro, Santa Catarina (28° 47′ 09″ S, 49° 39′ 23″ W). MCP 23638, 3 alc, rio Morto on road between Meleiro and São Francisco, *c.* 11 km north of Meleiro, Meleiro, Santa Catarina (28° 45′ 00″ S, 49° 39′ 29″ W). MCP 53973, 3 alc, 1 tis, rio Amola Faca at bridge on road SC-285 between Turvo and Timbé do Sul, Timbé do Sul, Santa Catarina (28° 50′ 25″ S, 49° 48′ 02″ W). MCN 4734, 4 alc, rio Jordão Baixo, tributary to rio Mãe Luzia, Siderópolis, Santa Catarina (28° 35′ 13″ S, 49° 29′ 20″ W). UFRGS 261, 1 alc, rio Jordão at Jordão Baixo, Siderópolis, Santa Catarina (28° 36′ 00.02″ S, 49° 24′ 57.60″ W). UFRGS 1861, 251 alc, rio Jordão at Jordão Baixo, Siderópolis, Santa Catarina (*c.* 28° 36′ S, 49° 25′ W). UFRGS 6111, 60 alc, rio Mãe Luzia, Treviso, Santa Catarina (28° 27′ 58″ S, 49° 28′ 18″ W). UFRGS 6214, 9 alc, rio Mãe Luzia at Mina Comim, Treviso, Santa Catarina. UFRGS 10863, 12 alc, rio do Salto at Parque Ecológico, Timbé do Sul, Santa Catarina (28° 49′ 44″ S, 49° 45′ 21″ W). UFRGS 12544, 1 alc, rio Jordão Alto, Nova Veneza, Santa Catarina (28° 39′ 29″ S, 49° 32′ 36″ W). UFRGS 15390, 9 alc, rio Mãe Luzia, Treviso, Santa Catarina (28° 28′ 00″ S, 49° 28′ 19″ W). UFRGS 22945, 3 alc, stream next to Alto Jordão, Nova Veneza, Santa Catarina (28° 35′ 02.2″ S, 49° 32′ 31.2″ W). UNICTIO 1866, 6 of 14 alc, 4 tis, stream on road to Vila Artesanal, tributary to rio Araranguá, Jacinto Machado, Parque Nacional Aparados da Serra, Santa Catarina (29° 01′ 47.8″ S, 49° 54′ 04.4″ W). UNICTIO 1882, 1 of 3 alc, 4 tis, arroio Pai José, tributary to rio Araranguá, Jacinto Machado, Santa Catarina (29° 00′ 42.6″ S, 49° 53′ 19.0″ W). *Epactionotus* sp. Urussanga: MCP 53836, 16 alc, 3 tis, creek tributary of rio Carvão Alto, Urussanga, Santa Catarina (28° 30′ 02.7″ S, 49° 23′ 10.0″ W). UFRGS 6212, 10 alc, rio Lageado near USITESC, Urussanga, Santa Catarina (28° 31′ 04.92″ S, 49° 19′ 10.07″ W). UFRGS 9060, 8 alc, creek tributary to rio Urussanga, Urussanga, Santa Catarina (28° 30′ 00.33″ S, 49° 23′ 43.00″ W). *Epactionotus* sp. d'Una: MCP 35156, 1 tis, stream tributary to rio d'Una, Imbituba, Santa Catarina (28° 11′ 56″ S, 48° 47′ 17″ W). MZUEL 07528, 51 alc, 5 tis, rio d'Una, Imarui, Santa Catarina (28° 10′ 48.8″ S, 48° 47′ 12.0″ W). *Epactionotus* sp. Tubarão: UFRGS 22941, 3 alc, 1 tis, rio Bonito, on Rio Bonito Alto, Santa Catarina (28° 25′ 48.3″ S, 49° 27′ 50.7″ W). MCN 18835, 4 alc, rio Palmeiras, tributary to rio Tubarão, Lauro Müller, Santa Catarina (28° 27′ 01″ S, 49° 25′ 03″ W). MCN 18844, 1 alc, rio do Rastro, tributary to rio Tubarão, Lauro Müller, Santa Catarina (28° 21′ 50″ S, 49° 26′ 43″ W).

## ACKNOWLEDGEMENTS

The authors are grateful to Carlos Lucena and Margarete Lucena for their continued support at the Laboratory of Ichthyology of MCP and to Luiz Malabarba and Juliana Wingert (UFRGS), Vinícius Bertaco (MCN) and Pablo Lehmann (UNICTIO) for the loan and donation of specimens and tissue samples. The authors thank Andréa Thomaz, Fernando Carvalho, Nathália Pio, Laura Donin and Juliano Ferrer for help in the collection of specimens of the new species. M.L.S.D. thanks Alejandro Londoño-Burbano, Bárbara B. Calegari, Rafael Lugo, Vinícius Lorini and Vanessa Meza for initial guidance in the molecular lab and amplifications; Juliano Romanzini for help with the microphotography in Figures 14 and 17; and Hernán López-Fernández and Nelson Rosa Fagundes for review and significant contributions to manuscript and analyses. M.L.S.D. is also grateful to Coordenação de Aperfeiçoamento de Pessoal de Nível Superior – Brasil (CAPES) for the doctoral fellowship (finance code 001) during which this project was developed and completed. Amplifications, sequencing and a field trip to collect specimens were accomplished with support from the Conselho Nacional de Desenvolvimento Científico e Tecnológico, CNPq (process number 40166/2016-0), to R.E.R. in which T.P.C. is a collaborator. R.E.R. is partially financed by CNPq (process number 306455/2014-5).

## AUTHOR CONTRIBUTIONS

M.L.S.D., T.P.C. and R.E.R. designed the study. R.E.R. and T.P.C. made substantial contributions to conception and acquisition of data. M.L.S.D. generated morphological and molecular data. M.L.S.D. and T.P.C. analysed the data. M.L.S.D., T.P.C. and R.E.R. interpreted the results and wrote the manuscript.

## ORCID

*Maria Laura S. Delapieve* https://orcid.org/0000-0003-2408-1733
*Tiago P. Carvalho* https://orcid.org/0000-0001-5901-1634
*Roberto E. Reis* https://orcid.org/0000-0003-3746-6894

## REFERENCES

Abell, R., Thieme, M. L., Revenga, C., Bryer, M., Kottelat, M., Bogutskaya, N., … Petry, P. (2008). Freshwater ecoregions of the world: a new map of biogeographic units for freshwater biodiversity conservation. *BioScience*, *58*, 403–414.

Aitchison, J. (1982). The statistical analysis of compositional data. *Journal of the Royal Statistical Society: Series B (Methodological)*, *44*, 139–177.

Albert, J. S., & Carvalho, T. P. (2011). Neogene assembly of modern faunas. In J. S. Albert & R. E. Reis (Eds.), *Historical biogeography of Neotropical freshwater fishes* (pp. 119–136). Berkeley, CA: University of California Press, Ltd..

Albert, J. S., Petry, P., & Reis, R. E. (2011). Major biogeographic and phylogenetic patterns. In J. S. Albert & R. E. Reis (Eds.), *Historical biogeography of Neotropical freshwater fishes* (pp. 21–57). Berkeley, CA: University of California Press, Ltd..

Anderson, M. J. (2001). A new method for non-parametric multivariate analysis of variance. *Austral Ecology*, *26*, 32–46.

Angrizani, R. C., & Malabarba, L. R. (2018). Morphology and molecular data reveal the presence of two new species under *Rhamdia quelen* (Quoy Gaimard, 1824) (Siluriformes: Heptapteridae) species complex. *Zootaxa*, *4388*, 41–60.

Benine, R. C., Mariguela, T. C., & Oliveira, C. (2009). New species of *Moenkhausia* Eigenmann, 1903 (Characiformes: Characidae) with comments on the *Moenkhausia oligolepis* species complex. *Neotropical Ichthyology*, *7*, 161–168.

Bermingham, E., McCafferty, S. S., & Martin, A. P. (1997). Fish biogeography and molecular clocks: Perspectives from the Panamanian isthmus. In T. D. Kocher & C. A. Stepien (Eds.), *Molecular systematics of fishes* (pp. 113–128). San Diego, CA: Academic Press.

Bertaco, V. A., Ferrer, J., Carvalho, F. R., & Malabarba, L. R. (2016). Inventory of the freshwater fishes from a densely collected area in South America-a case study of the current knowledge of Neotropical fish diversity. *Zootaxa*, *4138*, 401–440.

Bouckaert, R., Vaughan, T. G., Barido-Sottani, J., Duchêne, S., Fourment, M., Gavryushkina, A., … Drummond, A. J. (2019). BEAST 2.5: an advanced software platform for Bayesian evolutionary analysis. *PLoS Computational Biology*, *15*, e1006650.

Calegari, B. B., Delapieve, M. L. S., & Souza, L. M. (2016). Tutorial para preparação de mapas de distribuição geográfica. *Boletim Sociedade Brasileira de Ictiologia*, *118*, 15–30.

Calegari, B. B., Lehmann, P. A., & Reis, R. E. (2011). A new species of *Otothyropsis* (Siluriformes: Loricariidae) from the rio Paraguay basin, Paraguay. *Neotropical Ichthyology*, *9*, 253–260.

Calegari, B. B., Silva, E. V., & Reis, R. E. (2014). *Microlepidogaster discontenta*, a new species of hypoptopomatine catfish (Teleostei: Loricariidae) from the rio São Francisco basin, Brazil. *Ichthyological Exploration of Freshwaters*, *25*, 213–221.

Carvajal-Quintero, J., Villalobos, F., Oberdorff, T., Grenouillet, G., Brosse, S., Hugueny, B., … Tedesco, P. A. (2019). Drainage network position and historical connectivity explain global patterns in freshwater fishes' range size. *Proceedings of the National Academy of Sciences*, *116*, 13434–13439.

Carvalho, T. P. (2007). Distributional patterns of freshwater fishes in coastal Atlantic drainages of eastern Brazil: a preliminary study applying parsimony analysis of endemism. *Darwiniana*, *45*.65–67.

Carvalho, T. P., & Reis, R. E. (2011). Taxonomic review of *Hisonotus* Eigenmann & Eigenmann (Siluriformes: Loricariidae: Hypoptopomatinae) from the Laguna dos Patos system, southern Brazil. *Neotropical Ichthyology*, *9*, 1–48.

Cherobim, A. M., Lazzarotto, H., & Langeani, F. (2016). A new species of the catfish *Neoplecostomus* (Loricariidae: Neoplecostominae) from a coastal drainage in southeastern Brazil. *Neotropical Ichthyology*, *14*, e160015.

Chiachio, M. C., Oliveira, C., & Montoya-Burgos, J. I. (2008). Molecular systematic and historical biogeography of the armored Neotropical catfishes Hypoptopomatinae and Neoplecostominae (Siluriformes: Loricariidae). *Molecular Phylogenetics and Evolution*, *49*, 606–617.

Chuctaya, J., Bührnheim, C. M., & Malabarba, L. R. (2018). Two new species of *Odontostilbe* historically hidden under *O. microcephala* (Characiformes: Cheirodontinae). *Neotropical Ichthyology*, *16*, e170047.

Cramer, C. A., Bonatto, S. L., & Reis, R. E. (2011). Molecular phylogeny of the Neoplecostominae and Hypoptopomatinae (Siluriformes: Loricariidae) using multiple genes. *Molecular Phylogenetics and Evolution*, *59*, 43–52.

Cramer, C. A., Liedke, A. M. R., Bonatto, S. L., & Reis, R. E. (2007). The phylogenetic relationships of the Hypoptopomatinae and Neoplecostominae (Siluriformes: Loricariidae) as inferred from mitochondrial cytochrome c oxidase I sequences. *Bulletin of Fish Biology*, *9*, 51–59.

da Cruz, M. D. O., & Weksler, M. (2018). Impact of tree priors in species delimitation and phylogenetics of the genus *Oligoryzomys* (Rodentia: Cricetidae). *Molecular Phylogenetics and Evolution*, *119*, 1–12.

de Queiroz, K. (2007). Species concepts and species delimitation. *Systematic Biology*, *56*, 879–886.

Dagosta, F. C. P., & Pinna, M. D. (2017). Biogeography of Amazonian fishes: deconstructing river basins as biogeographic units. *Neotropical Ichthyology*, *15*, e170034.

Delapieve, M. L. S., Lehmann, P. A., & Reis, R. E. (2017). An appraisal of the phylogenetic relationships of Hypoptopomatini cascudinhos with description of two new genera and three new species (Siluriformes: Loricariidae). *Neotropical Ichthyology*, *15*, e170079.

Edgar, R. C. (2004). MUSCLE: multiple sequence alignment with high accuracy and high throughput. *Nucleic Acids Research*, *32*, 1792–1797.

Ezard, T., Fujisawa, T., Barraclough, T. G. (2009). Splits: Species' Limits by Threshold Statistics. R package version 1.0-11/r29. http://www.R-Forge.R project.org/projects/splits

Fagundes, P. C., Pereira, E. H. L., & Reis, R. E. (2020). Iterative taxonomic study of *Pareiorhaphis hystrix* (Siluriformes, Loricariidae) suggests a single, yet phenotypically variable, species in South Brazil. *PLoS ONE*, *15*, e0237160.

Faustino-Fuster, D. R., Bockmann, F. A., & Malabarba, L. R. (2019). Two new species of *Heptapterus* (Siluriformes: Heptapteridae) from the Uruguay River basin, Brazil. *Journal of Fish Biology*, *94*, 352–373.

Ferrer, J., Donin, L. M., & Malabarba, L. R. (2015). A new species of *Ituglanis* Costa & Bockmann, 1993 (Siluriformes: Trichomycteridae) endemic to the Tramandaí-Mampituba ecoregion southern Brazil. *Zootaxa*, *4020*, 375–389.

Fujisawa, T., & Barraclough, T. G. (2013). Delimiting species using single-locus data and the generalized mixed yule coalescent approach: a revised method and evaluation on simulated data sets. *Systematic Biology*, *62*, 707–724.

Gauger, M. F. W., & Buckup, P. A. (2005). Two new species of Hypoptopomatinae from the rio Paraíba do Sul basin, with comments on the monophyly of *Parotocinclus* and the Otothyrini (Siluriformes: Loricariidae). *Neotropical Ichthyology*, *3*, 509–518.

Guisande, C., Vari, R. P., Heine, J., García-Roselló, E., González-Dacosta, J., Perez-Schofield, G. J. B., … Pelayo-Villamil, P. (2016). VARSEDIG: an algorithm for morphometric characters selection and statistical validation in morphological taxonomy. *Zootaxa*, *4162*, 571–580.

Hammer, Ø., Harper, D. A. T., & Ryan, P. D. (2001). PAST: Paleontological statistics software package for education and data analysis. *Palaeontologia Electronica*, *4*, 1–9.

Harvey, M. G., Seeholzer, G. F., Smith, B. T., Rabosky, D. L., Cuervo, A. M., & Brumfield, R. T. (2017). Positive association between population genetic differentiation and speciation rates in New World birds. *Proceedings of the National Academy of Sciences*, *114*, 6328–6333.

Hirschmann, A., Fagundes, N. J., & Malabarba, L. R. (2017). Ontogenetic changes in mouth morphology triggers conflicting hypotheses of relationships in characid fishes (Ostariophysi: Characiformes). *Neotropical Ichthyology*, *15*, e160073.

Hirschmann, A., Malabarba, L. R., Thomaz, A. T., & Fagundes, N. J. R. (2015). Riverine habitat specificity constrains dispersion in a Neotropical fish (Characidae) along southern Brazilian drainages. *Zoologica Scripta*, *44*, 374–382.

IUCN Standards and Petitions Committee. (2019). Guidelines for using the IUCN Red List Categories and Criteria. Version 14. Prepared by the Standards and Petitions Committee. Available at: http://www.iucnredlist.org/documents/RedListGuidelines.pdf

Kearse, M., Moir, R., Wilson, A., Stones-Havas, S., Cheung, M., Sturrock, S., … Drummond, A. (2012). Geneious basic: an integrated and extendable desktop software platform for the organization and analysis of sequence data. *Bioinformatics*, *28*, 1647–1649.

Kimura, M. (1980). A simple method for estimating evolutionary rate of base substitutions through comparative studies of nucleotide sequences. *Journal of Molecular Evolution*, *16*, 111–120.

Kumar, S., Stecher, G., & Tamura, K. (2016). MEGA7: molecular evolutionary genetics analysis version 7.0 for bigger datasets. *Molecular Biology and Evolution*, *33*, 1870–1874.

Lanfear, R., Frandsen, P. B., Wright, A. M., Senfeld, T., & Calcott, B. (2016). PartitionFinder 2: new methods for selecting partitioned models of evolution for molecular and morphological phylogenetic analyses. *Molecular Biology and Evolution*, *34*, 772–773.

Leal, M. E. C., & Sant'Anna, V. B. (2006). Quantitative analysis of interspecific and ontogenetic variation in *Osteoglossum* species (Teleostei: Osteoglossiformes: Osteoglossidae). *Zootaxa*, *1239*, 49–68.

Leigh, J. W., & Bryant, D. (2015). Monte Carlo strategies for selecting parameter values in simulation experiments. *Systematic Biology*, *64*, 741–751.

Lima, S. M., Berbel-Filho, W. M., Araújo, T. F., Lazzarotto, H., Tatarenkov, A., & Avise, J. C. (2017). Headwater capture evidenced by paleo-rivers reconstruction and population genetic structure of the armored catfish (*Pareiorhaphis garbei*) in the Serra Do Mar mountains of southeastern Brazil. *Frontiers in Genetics*, *8*, 1–8.

Lippert, B. G., Calegari, B. B., & Reis, R. E. (2014). A new species of *Otothyropsis* (Siluriformes: Hypoptopomatinae) from eastern Brazil. *Copeia*, *2*, 238–244.

Malabarba, L. R., & Isaia, E. A. (1992). The fresh water fish fauna of the rio Tramandaí drainage, Rio Grande do Sul, Brazil, with a discussion of its historical origin. *Comunicações do Museu de Ciências e Tecnologia da PUCRS, Série Zoologia*, *5*, 197–223.

Malabarba, L. R., Carvalho Neto, P., Bertaco, V. A., Carvalho, T. P., Ferrer, J., & Artioli, L. G. S. (2013). *Guia de Identificação dos Peixes da Bacia do Rio Tramandaí*. Porto Alegre, Brazil: Via Sapiens.

Martins, F. O., Britski, H. A., & Langeani, F. (2014). Systematics of *Pseudotothyris* (Loricariidae: Hypoptopomatinae). *Zoological Journal of Linnean Society*, *170*, 822–874.

Melo, B. F., Benine, R. C., Mariguela, T. C., & Oliveira, C. (2011). A new species of *Tetragonopterus* Cuvier, 1816 (Characiformes: Characidae: Tetragonopterinae) from the rio Jari, Amapá, northern Brazil. *Neotropical Ichthyology*, *9*, 49–56.

Pereira, E. H. L., Vieira, F., & Reis, R. E. (2007). A new species of sexually dimorphic *Pareiorhaphis* Miranda Ribeiro, 1918 (Siluriformes: Loricariidae) from the rio Doce Basin, Brazil. *Neotropical Ichthyology*, *5*, 443–448.

QGIS Development Team. (2020). Geographic Information System (QGIS). Open Source Geospatial Foundation Project. http://www.qgis.org/.

R Core Team. (2013). R: A Language and Environment for Statistical Computing. R Foundation for Statistical Computing, Vienna. Available at: http://www.R-project.org/

Rambaut, A., Drummond, A. J., Xie, D., Baele, G., & Suchard, M. A. (2018). Posterior summarisation in Bayesian phylogenetics using tracer 1.7. *Systematic Biology*, *67*, 901–904.

Reis, R. E., & Schaefer, S. A. (1998). New cascudinhos from southern Brazil: systematics, endemism, and relationships (Siluriformes, Loricariidae, Hypoptopomatinae). *American Museum Novitates*, *3254*, 1–25.

Ribeiro, A. C. (2006). Tectonic history and the biogeography of the freshwater fishes from the coastal drainages of eastern Brazil: an example of faunal evolution associated with a divergent continental margin. *Neotropical Ichthyology*, *4*, 225–246.

Rodriguez, M. S., Delapieve, M. L. S., & Reis, R. E. (2015). Phylogenetic relationships of the species of *Acestridium* Haseman, 1911 (Siluriformes: Loricariidae). *Neotropical Ichthyology*, *13*, 325–340.

Roxo, F. F., Albert, J. S., Silva, G. S., Zawadzki, C. H., Foresti, F., & Oliveira, C. (2014). Molecular phylogeny and biogeographic history of the armored Neotropical catfish subfamilies Hypoptopomatinae, Neoplecostominae and Otothyrinae (Siluriformes: Loricariidae). *PLoS One*, *9*, e105564.

Roxo, F. F., Lujan, N. K., Tagliacollo, V. A., Waltz, B. T., Silva, G. S., Oliveira, C., & Albert, J. S. (2017). Shift from slow-to fast-water habitats accelerates lineage and phenotype evolution in a clade of Neotropical suckermouth catfishes (Loricariidae: Hypoptopomatinae). *PLoS One*, *12*, e0178240.

Roxo, F. F., Ochoa, L. E., Sabaj, M. H., Lujan, N. K., Covain, R., Silva, G. S., … Alfaro, M. E. (2019). Phylogenomic reappraisal of the Neotropical catfish family Loricariidae (Teleostei: Siluriformes) using ultraconserved elements. *Molecular Phylogenetics and Evolution*, *135*, 148–165.

RStudio Team. (2020). *RStudio: Integrated development for R. RStudio*. Boston, MA: PBC. Retrieved from http://www.rstudio.com/.

Sabaj M.H. 2019. Standard symbolic codes for institutional resource collections in herpetology and ichthyology: An Online Reference. Version 7.1. Washington, DC: American Society of Ichthyologists and Herpetologists. Retrieved from www.asih.org/.

Schaefer, S. A. (1997). The Neotropical cascudinhos: systematics and biogeography of the *Otocinclus*, catfishes (Siluriformes: Loricariidae). *Proceedings of the Academy of Natural Sciences of Phyladelphia*, *148*, 1–120.

Schaefer, S. A. (1998). Conflict and resolution: Impact of new taxa on phylogenetic studies of the Neotropical cascudinhos (Siluroidei: Loricariidae). In L. R. Malabarba, R. E. Reis, R. P. Vari, Z. M. Lucena, & C. A. S. Lucena (Eds.), *Phylogeny and classification of Neotropical fishes* (pp. 375–400). Porto Alegre, Brazil: Edipucrs.

Singhal, S., Huang, H., Grundler, M. R., Marchán-Rivadeneira, M. R., Holmes, I., Title, P. O., … Rabosky, D. L. (2018). Does population structure predict the rate of speciation? A comparative test across Australia's most diverse vertebrate radiation. *The American Naturalist*, *192*, 432–447.

Talavera, G., Dincă, V., & Vila, R. (2013). Factors affecting species delimitations with the GMYC model: insights from a butterfly survey. *Methods in Ecology and Evolution*, *4*, 1101–1110.

Taylor, W. R., & Van Dyke, G. C. (1985). Revised procedures for staining and clearing small fishes and other vertebrates for bone and cartilage study. *Cybium*, *9*, 107–119.

Thomaz, A. T., & Knowles, L. L. (2018). Flowing into the unknown: inferred paleodrainages for studying the ichthyofauna of Brazilian coastal rivers. *Neotropical Ichthyology*, *16*, e180019.

Thomaz, A. T., & Knowles, L. L. (2020). Common barriers, but temporal dissonance: genomic tests suggest ecological and paleo-landscape sieves structure a coastal riverine fish community. *Molecular Ecology*, *29*, 783–796.

Thomaz, A. T., Malabarba, L. R., Bonatto, S. L., & Knowles, L. L. (2015). Testing the effect of palaeodrainages versus habitat stability on genetic divergence in riverine systems: study of a Neotropical fish of the Brazilian coastal Atlantic Forest. *Journal of Biogeography*, *42*, 2389–2401.

Thomaz, A. T., Malabarba, L. R., & Knowles, L. L. (2017). Genomic signatures of paleodrainages in a freshwater fish along the southeastern coast of Brazil: genetic structure reflects past riverine properties. *Heredity*, *119*, 287–294.

Wendt, E. W., Silva, P. C., Malabarba, L. R., & Carvalho, T. P. (2019). Phylogenetic relationships and historical biogeography of *Oligosarcus* (Teleostei: Characidae): examining riverine landscape evolution in southeastern South America. *Molecular Phylogenetics and Evolution*, *140*, 106604.

## SUPPORTING INFORMATION

Additional supporting information may be found online in the Supporting Information section.

**How to cite this article:** Delapieve MLS, Carvalho TP, Reis RE. Species delimitation in a range-restricted group of cascudinhos (Loricariidae: *Epactionotus*) supports morphological and genetic differentiation across coastal rivers of southern Brazil. *J Fish Biol*. 2020;97:1748–1769. https://doi.org/10.1111/jfb.14538